OULU 2021
C 804

ACTA UNIVERSITATIS OULUENSIS


*Leo-Juhani Meriö*

# OBSERVATIONS AND ANALYSIS OF SNOW COVER AND RUNOFF IN BOREAL CATCHMENTS

*UNIVERSITY OF OULU GRADUATE SCHOOL;*
*UNIVERSITY OF OULU,*
*FACULTY OF TECHNOLOGY*

ACTA UNIVERSITATIS OULUENSIS
C Technica 804

*LEO-JUHANI MERIÖ*

# OBSERVATIONS AND ANALYSIS OF SNOW COVER AND RUNOFF IN BOREAL CATCHMENTS

Academic dissertation to be presented with the assent of the Doctoral Training Committee of Technology and Natural Sciences of the University of Oulu for public defence in the OP auditorium (L10), Linnanmaa, on 19 November 2021, at 12 noon

UNIVERSITY OF OULU, OULU 2021

Acta Univ. Oul. C 804, 2021

Supervised by
Assistant Professor Hannu Marttila
Professor Bjørn Kløve
Doctor Pertti Ala-aho

Reviewed by
Professor Sean Carey
Assistant Professor David Finger

Opponent
Professor Hjalmar Laudon

ISBN 978-952-62-3064-1 (Paperback)
ISBN 978-952-62-3065-8 (PDF)

ISSN 0355-3213 (Printed)
ISSN 1796-2226 (Online)

Cover Design
Raimo Ahonen

PUNAMUSTA
TAMPERE 2021

**Meriö, Leo-Juhani, Observations and analysis of snow cover and runoff in boreal catchments.**
University of Oulu Graduate School; University of Oulu, Faculty of Technology
*Acta Univ. Oul. C 804, 2021*
University of Oulu, P.O. Box 8000, FI-90014 University of Oulu, Finland

***Abstract***

Snow conditions in the boreal region are changing, mainly due to climate change. Snowmelt impacts catchment water storage conditions and streamflow through spring and early summer, and thus drastic changes in hydrological conditions are expected, especially in headwaters. The measurement of snow cover variability in the catchment scale is a challenge using current techniques, and the connections between catchment characteristics, climate conditions, and hydrology are still not completely understood. This thesis aims to develop and test new robust and cost-efficient observation methods to quantify and analyze snow cover variability and improve understanding of the factors controlling snow hydrology in the boreal landscape.

This work applies two approaches for measuring snow cover: in-situ, using low-cost temperature loggers; and remote sensing, using unmanned aerial systems with Structure-from-Motion (UAS-SfM). The high temporal-resolution data from temperature loggers, with the algorithm developed, provided relatively reliable and accurate data on spatiotemporal variations in snow cover ablation and melt rates in different boreal landcover types. The UAS-SfM method captured the snow depth variability in the boreal landscape throughout the snow season with a very high spatial resolution with a larger coverage area, enabling the identification of multiple snow processes and interactions between snow and vegetation.

To analyze the factors controlling snow hydrology, data from a spatially well-represented Finnish small-basing research network was used to calculate low flows and catchment storage indices using the recession analysis method. The findings suggest that the changes in summer low flow related to snow conditions will be pronounced in certain snow-to-precipitation ratio thresholds in a warming climate, highlighting the strong connection between ecologically important summer low flows and snow conditions.

The developed measurement methods can be used in measuring snowpack variations in ungauged or remote basins and, especially with the data from UAS-SfM, in extending snow course measurements and improving distributed catchment-scale snow models. The improved understanding of the factors controlling snow hydrology can be used to guide water resource and land-use management in boreal and high-latitude regions, where rapid climate change is projected.

*Keywords:* catchment storage, high resolution, observation methods, runoff, snow

**Meriö, Leo-Juhani, Lumipeitteen mittausmenetelmät ja analyysi sekä vaikutukset pohjoisten latvavesistöjen virtaamiin.**
Oulun yliopiston tutkijakoulu; Oulun yliopisto, Teknillinen tiedekunta
*Acta Univ. Oul. C 804, 2021*
Oulun yliopisto, PL 8000, 90014 Oulun yliopisto

## *Tiivistelmä*

Pohjoiset lumiolosuhteet ovat muuttumassa erityisesti ilmastonmuutoksen takia. Lumen sulanta vaikuttaa valuma-alueiden vesivarastoihin ja virtaamiin keväällä ja alkukesästä, ja hydrologisten olosuhteiden odotetaan muuttuvan rajusti erityisesti latvavesistössä. Lumipeitteen vaihtelun mittaaminen valuma-alueilla on nykyisillä menetelmillä haastavaa ja tiedot valuma-aluetekijöiden, ilmasto-olosuhteiden ja hydrologisten olosuhteiden välisistä yhteyksistä ovat puutteellisia. Tässä työssä kehitetään ja testataan uusia kustannustehokkaita havaintomenetelmiä lumipeitteen vaihtelun mittaamiseen ja analysointiin sekä pyritään parantamaan ymmärrystä lumihydrologiaa ohjaavista tekijöistä pohjoisilla alueilla.

Lumipeitteen mittausta lähestytään maastohavainnoin käyttämällä kustannustehokkaita lämpötila-antureita ja kaukokartoituksen avulla käyttäen miehittämättömiä lennokkeja yhdessä Structure-from-Motion (UAS-SfM) fotogrammetrian kanssa. Lämpötila-antureilla mitatun korkean resoluution datan ja kehitetyn algoritmin avulla saatiin suhteellisen tarkkaa tietoa lumen prosessien vaihteluista pohjoisilla maastotyypeillä. UAS-SfM menetelmällä lumen syvyyden alueellinen vaihtelu määritettiin erittäin suurella resoluutiolla kattaen suuremman alueen, joka mahdollisti useiden lumen prosessien sekä lumen ja kasvillisuuden vuorovaikutusten tunnistamisen.

Lumihydrologiaa ohjaavien tekijöiden selvittämiseen käytettiin alueellisesti hyvin jakautuneiden Suomen pienvaluma-alueiden dataa, josta laskettiin alivirtaamat, ja vesivarastoindeksejä käyttäen resessioanalyysiä. Tulokset viittasivat lämpenevässä ilmastossa muuttuvien lumiolosuhteiden vaikuttavan kesän alivirtaamiin erityisen voimakkaasti alueilla, joissa lumen osuus vuosittaisesta kokonaissadannasta on tietyllä kynnyksellä, korostaen ekologisesti tärkeiden kesän alivirtaamien ja lumiolosuhteiden voimakasta yhteyttä.

Työssä testattuja ja kehitettyjä mittausmenetelmiä voidaan käyttää lumipeitteen vaihtelun määrittämiseen etäisillä tai mittaamattomilla valuma-alueilla. Erityisesti UAS-SfM menetelmä soveltuu laajentamaan lumilinjamittausten alueellista kattavuutta ja parantamaan hajautettuja valuma-aluetason lumimalleja. Työssä tuotettua uutta tietoa lumihydrologiaa ohjaavista tekijöistä voidaan hyödyntää vesistöjen ja maankäytön hallintaan ja suunnitteluun pohjoisilla alueilla, joilla ilmastonmuutoksen on ennustettu olevan nopeaa.

*Asiasanat:* korkea resoluutio, lumi, mittausmenetelmät, valuma-alueen vesivarasto, virtaama

*To my family and friends*

# Acknowledgements

I have been privileged to walk alongside people with exceptionally warm-hearts, friendliness, openness, and awesomeness, not to mention the knowledge and wisdom, during this journey. My sincere gratitude goes to Professor Bjørn Kløve for supervision, guidance, and accepting me as a PhD student in his research group. Warm thanks also to Assistant Professor Hannu Marttila and Dr. Pertti Ala-aho for their valuable advice, detailed comments on manuscripts, encouragement, and support throughout my studies. Special thanks to Hannu for taking over the main supervision during the process. I would like to thank Pekka Hänninen, Jarkko Okkonen, Raimo Sutinen, Jan Hjort, Jarmo Linjama, Pasi Korpelainen, Anton Kuzmin, Anssi Rauhala and Timo Kumpula for fluent research co-operation that made the articles and finally this thesis possible. I also thank the members of my follow-up group: Prof. Anne Tolvanen, Prof. Jukka Hast and Dr. Anna-Kaisa Ronkanen for their valuable contribution to my work. I would like to thank Professor Sean Carey and Assistant Professor David Finger for their efforts in pre-examining this thesis and Mary McAfee and Will Cowley for checking the language of my articles and this thesis. Jenni, thank you for the discussions bringing brightness and clarity to my life in the late phase of this work.

I would like to thank Maa- ja vesitekniikan tuki ry for essential funding for this work, and additional travel grants. Without your support this work and attending several international scientific conferences and courses would not have been possible. In addition, I appreciate the personal grants from Tauno Tönning Research Foundation and Sven Hallin Research Foundation. I would also like to acknowledge University of Oulu Graduate School for providing the framework and high-level education required for the studies.

Field work was a considerable part of this thesis and would not have been possible without help. Thank you Pertti and Essi-Maaria Ala-aho, Tuomo Reinikka, Veikko Pekkala, Romain Boche, Elodie Jacquel, Filip Muhic, Anna Jaros, Kashif Noor, Anton Kuzmin, Pasi Korpelainen, Aleksi Ritakallio, Timo Kumpula, Anssi Rauhala, Alexandre Pepy, Jari-Pekka Nousu, Tuomo Pitkänen and Valtteri ”The King in the North” Hyöky for the long days and sometimes nights spend mainly in the snowy north.

To all my awesome co-workers and colleagues especially in the Water, Energy, and Environmental Engineering Research group, greatest thanks for creating such an encouraging working atmosphere, for the vivid coffee room discussions, support, and warm treatment.

Lonely and dark can the world be without friends. Thank you for sharing your life with me and bringing balance to the Force. Peace and Love.

Finally, love and gratitude to my father, who passed away in spring 2020, I miss you so much. To my mother and sisters, for your support, encouragement, and being there. Thank you Sanna, my life partner, for your love and taking care of almost everything when I was busy with other things. Love that I cannot express with any acts or words to my sons, Aleksi and Lassi.

Oulu, September 2021 Leo-Juhani Meriö

# Abbreviations

| | |
|---|---|
| CV | Coeffifient of variation |
| ddf | Degree-day factor |
| DEM | Digital elevation model |
| DoD | DEM of differences |
| DOY | Day of the year |
| DSM | Digital surface model |
| GAM | Generalized additive model |
| GNSS | Global navigation satellite system |
| GPS | Global positioning system |
| LiDAR | Light detection and ranging |
| LOOCV | Leave-one-out cross-validation |
| MASL | Meters above sea level |
| PC | Principal component |
| PCA | Principal component analysis |
| PET | Potential evapotranspiration |
| P/PET | Wetness index |
| S/P | Snow to precipitation ratio |
| RTK | Real-time kinematic |
| SD | Snow depth |
| SfM | Surface-from-motion |
| SWE | Snow water equivalent |
| TDR | Time-domain-reflectometer |
| UAS | Unmanned aerial system |
| UAV | Unmanned aerial vehicle |

# List of original publications

This thesis is based on the following publications, which are referred to throughout the text by their Roman numerals:

I Meriö, L.-J., Marttila, H., Ala-aho, P., Hänninen, P., Okkonen, J., Sutinen, R., & Kløve, B. (2018). Snow profile temperature measurements in spatiotemporal analysis of snowmelt in a subarctic forest-mire hillslope. *Cold Regions Science and Technology, 151,* 119–132. https://doi.org/10.1016/j.coldregions.2018.03.013

II Meriö, L.-J., Rauhala, A., Ala-aho, P., Kuzmin, A., Korpelainen, P.,Kumpula, T., Kløve, B., & Marttila, H. (2021). Spatiotemporal variability of snow depth in subarctic environment using unmanned aircraft systems, Part 2: Snow processes and snow-canopy interactions. Manuscript.

III Meriö, L.-J., Ala-aho, P., Linjama, J., Hjort, J., Kløve, B., & Marttila, H. (2019). Snow to precipitation ratio controls catchment storage and summer flows in boreal headwater catchments. *Water Resources Research, 55*(5), 4096–4109. https://doi.org/10.1029/2018wr023031

The author's contribution to Papers I–III was as follows:

I Designed the study with supervisors. Performed the fieldwork with Pertti Ala-aho and performed the data analysis. Wrote the paper with co-authors.

II Designed the study with Anssi Rauhala and with guidance from supervisors. Performed fieldwork with co-authors. Analyzed the data and wrote the paper with co-authors. Performed the snow process analysis with critical and helpful comments from supervisors.

III Designed the study with guidance from supervisors. Collected the data and performed the analysis. Wrote the paper with co-authors. Received critical and helpful comments and formulation of the statistical methodology from supervisors and co-authors.

# Contents

# 1 Introduction

The boreal forest is one of the largest terrestrial biomes on earth and, with seasonal snow and ice cover, it has global scale impacts on carbon and energy balance and water cycles (Bonan et al., 1992; Dixon et al., 1994; Gauthier et al., 2015). Seasonal snow cover is vital for the ecosystem and cultures of the boreal forest, providing shelter for plants and animals in cold winter conditions (Aitchison, 2001; Blume-Werry et al., 2016), representing a major component of the hydrological cycle by maintaining freshwater resources (Mankin et al., 2015; Woo et al., 2008), and supporting recreational outdoor activities (Neuvonen et al., 2015; Scott et al., 2008). Moreover, about one-sixth of the Earth's population is reliant on the water supply provided by the meltwater from snow. The financial importance of potential snow cover change has been indicated to be in the order of trillions of dollars (Barnett et al., 2005; Sturm et al., 2017).

Changes in boreal snow cover have already been observed, with reduced snow depth, extent, and mass (Brown & Robinson, 2011; Luomaranta et al., 2019; Mudryk et al., 2020; Pulliainen et al., 2020), snowmelt of the shallower snowpack happening earlier, and thus slower (Luomaranta et al., 2019; Musselman et al., 2017), and decreased snowfall-to-rainfall ratios (Berghuijs et al., 2014). These changes are predicted to continue in the future (Räisänen, 2016; Räisänen & Eklund, 2012; Woo et al., 2008) and the total annual precipitation is predicted to increase in circumpolar areas (Stocker et al., 2014).

Together with direct human actions, such as deforestation (Kelly et al., 2016; Sørensen et al., 2009), groundwater abstraction (Konikow & Kendy, 2005; Wada et al., 2010), and catchment drainage actions (Holden et al., 2004; Prévost et al., 1999), the changes in snow cover can have critical consequences for ecologically important summer low flows (Poff et al., 1997), water security (Barnett et al., 2005; Castle et al., 2014; Musselman et al., 2017) and water quality (Price, 2011; Whitehead et al., 2009). Therefore, improved knowledge of snow conditions and the factors affecting the resilience of streamflow have high ecological, societal, scientific, and economic value and give important information for rational decision making.

## 1.1 Snow observations and measurements

Observations of snowpack are required to record, investigate, and predict the snow accumulation and melt. Measurement methods can be roughly divided into in-situ

or near-surface measurements, and remotely sensed measurements (Haberkorn, 2019). The former are usually needed to validate the latter. In-situ measurements of the macrostructure of snow, such as snow depth (SD) and snow water equivalent (SWE), are traditionally performed manually, using snow stakes and tubes (Kinar & Pomeroy, 2015; Kuusisto, 1984). Snow courses have been established to improve the poor representativeness of the single point measurements. They are typically 2–4 km long, permanently positioned transects in a given area, with measurement points every 50 m. Snow depth is measured at each point and density every 5$^{th}$ point, representing the snow conditions for different land cover and topography. However, the small-scale variability of snow cover is not captured using these techniques. To speed up and improve the spatial coverage of the rather slow and laborious snow depth measurements, a semi-automated MagnaProbe has been developed (Sturm & Holmgren, 2018). It consists of electronics including positioning unit, a steel rod, and a sliding basket with a magnet assembly. When the rod is pushed into the snow, the basket floats on the snow and the distance between the rod tip and magnet is measured and stored with the position data. Ground-penetrating radar has also been used to improve the spatial coverage of the snow depth and SWE measurement data (Gusmeroli & Grosse, 2012; Webb, 2017).

Automated sensors, such as snow pillows, gamma radiation-based sensors, lysimeters, digital cameras, and acoustic sensors, have been deployed to improve the temporal resolution of the data (Kinar & Pomeroy, 2015). A network of automated ultrasonic sensors can provide more representative data from varying physiographical conditions (Rice & Bales, 2010). However, it is common for the current in-situ measurements to be laborious and costly when reliable and high spatial coverage is required (Lundberg et al., 2010). Furthermore, the snow depth and melt rates should be measured in multiple locations for different topography and vegetation, even in small catchments (Kumar et al., 2016). Thus, new simple and robust measurement methods, especially to produce point and spatially comprehensive snowmelt rate estimates are needed.

Remote sensed satellite-based observations provide substantially greater spatial coverage of snow conditions and are important for investigating the role of snow in Earth's climate system, calibrating hydrological models and assessing water resources in remote areas (Dietz et al., 2012; Finger, 2018; Finger et al., 2015; Nolin, 2011), but the uncertainty is high, especially in forested areas (Cohen et al., 2015), and ground in-situ validation is needed (Kinar & Pomeroy, 2015). Moreover, the spatial resolution of the mature satellite-based SD and SWE products is coarse (~25 km) while higher resolution techniques are continuously under development

(Lievens et al., 2019; Sturm, 2015). To bridge the gap between in-situ and remote sensed snow depth data, manned aircrafts equipped with airborne light detection and ranging (LiDAR) have been deployed to acquire high-resolution snow depth data for relatively large areas. These do, however, come with high cost (Deems et al., 2013; Deems & Painter, 2006).

With a substantially lower cost, recently popularized Unmanned Aerial System with Structure from Motion (UAS-SfM) techniques have shown the potential for high-resolution snow depth mapping with a relatively large coverage (Vander Jagt et al., 2015). Recently, UAS-SfM studies (Buhler et al., 2016; Harder et al., 2020; Lendzioch et al., 2016; Niedzielski et al., 2019; Redpath et al., 2018; Walker et al., 2020) have focused on testing the accuracy of the method on mountainous regions or snow on tundra, glaciers, prairies, and meadows with mostly low (grassland, shrub, bushes) or non-vegetated surfaces, and the analysis is mostly done based on a single survey in the snowy season, or several surveys during melt period. Thus, there is a gap in testing the UAS-SfM based snow mapping and investigating snow accumulation and ablation processes and interactions between vegetation and snow in the boreal region throughout the whole winter season.

## 1.2 Snow accumulation and redistribution

The distribution of accumulated snow and its inter-annual variability is high and governed by climate and atmospheric conditions, together with terrain characteristics and vegetation in scales above 100 m. Additionally, wind transport, microtopography, and canopy interception are important in scales below 100 m (Jost et al., 2007; Liston & Sturm, 1998; McKay & Male, 1981; Pomeroy et al., 2002; Vajda et al., 2006; Winstral & Marks, 2014). The most important climate factors are temperature and wind that determine the structure of the falling snow and its redistribution near the surface (Rasmus, 2005) where the distribution of snow is dependent on the terrain properties and vegetation.

In subtle topography, the vegetation can be the primary control of snow depth variability (Link & Marks, 1999). Forested and open areas have been found to have different snow processes (Gelfan et al., 2004). Wind transportation is hindered in forested areas, where the wind speeds are reduced while the snow is redistributed and eroded more freely in larger open areas, leading to sublimation during transport and reduced snow accumulation (Hiemstra et al., 2002). The edges of the open areas act as a sink for the drifted snow. In forests, the snow-canopy interactions, such as canopy interception and sublimation, affect the snow accumulation patterns

with less snow in denser coniferous forests (Hedstrom & Pomeroy, 1998; Pomeroy & Gray, 1995; Varhola et al., 2010). Moreover, forest openings and their size has been found to affect snow depth, with more snow on clearings 2–5 times the height of the surrounding trees (Pomeroy et al., 2002). Even though the snow accumulation processes and the factors impacting it have been studied extensively, the complex interactions between climate, terrain conditions, and vegetation make it difficult to get representative data from the snow cover or model the spatiotemporal evolution of the snow cover. Thus, more detailed high-resolution information on snow accumulation and melt is needed to support process understanding, modeling, forecast, and decision making.

## 1.3 Snowmelt and runoff processes

Seasonal snowmelt dominates the hydrological processes in high latitude and boreal regions. Over winter, falling snow accumulates on the ground, forming a large storage of water which is then released during spring freshet, causing high flows and frequent floods, affecting soil moisture, recharging groundwater, and sustaining low flow in early summer (Earman et al., 2006; Godsey et al., 2014; Kinar & Pomeroy, 2015; Okkonen & Kløve, 2011). The snowmelt is governed by the meteorological forcing, influenced mainly by topography and vegetation, that determine the available energy for melt (Jost et al., 2007). Snowmelt rates are generally lower in areas that are protected from direct sunlight, like northern slopes, topographic depressions, and areas shaded by dense canopies (Clark et al., 2011; Gary, 1974; Talbot et al., 2006).

Increased melt speeds have been observed near forest canopies that absorb incoming solar radiation, due to their low albedo compared to snow, and reflecting long-wave radiation to its surrounding areas (Golding & Swanson, 1978; Link & Marks, 1999; Pomeroy & Dion, 1996). In addition to energy balance, the timing of snow cover depletion has been observed to depend on the amount of pre-melt snow (Faria et al., 2000; Liston, 1999). Further reduced snowmelt rates are predicted because of the earlier snowmelt due to climate change, causing less energy to be available for the melt (Musselman et al., 2017). This creates a potential mismatch between supply and demand of the water and declined stream flows because snowmelt water is lost to streams before the vegetation growth period and when the evapotranspiration demand is highest.

In addition to the timing, speed, and magnitude of the meltwater from snow, the physiographical and vegetation characteristics of catchments determine their

storage properties and the runoff dynamics that influence the infiltration, groundwater storage, water release, and evapotranspiration (Blöschl et al., 2013; Price, 2011). The catchment characteristics developed under complex interactions between topography, soil, vegetation under the influence of climate and geological processes, such as weathering and erosion. These, together with climate, determine the catchment's sensitivity to change (Blöschl et al., 2013; Woods, 2005). Small headwater catchments are especially vulnerable to climate and human influences (Finn et al., 2011).

Landscape characteristics such as thick glacial till deposits, peatland/wetland areas, forest on sandy soils, and glaciofluvial deposits have been shown to promote water storage and low flows, while shallow till, hummocky moraines, deciduous-mixed wood forest, and open-water wetlands have been shown to have the opposite effect (Buttle & Eimers, 2009; Devito et al., 2017; Karlsen et al., 2016). The topographical control over baseflow has been shown to decrease during the recession, indicating that catchment subsurface properties then gain importance (Payn et al., 2012). Depending on peatland location and type, natural groundwater levels, and time since drainage operations, peatland drainage has been shown to both increase and decrease catchment storage and low flows (Bacon et al., 2017; Holden et al., 2004).

Summer low flows are significantly influenced by topography in snow-dominated catchments (Li et al., 2018) and are strongly dependent on annual peak snow water equivalent (Godsey et al., 2014), as well as precipitation after peak SWE (Jenicek et al., 2016). Elevation and topography have been found to influence catchment storage (Staudinger et al., 2017) and low flows (Li et al., 2018) in mountainous catchments. However, no previous study has examined the combined influence of catchment characteristics and climate, particularly snow conditions, on catchment storage and its sensitivity to change and low flows in boreal regions.

## 1.4 Objectives of this study

The main aim of this thesis was to gain an understanding of the factors controlling snow hydrology in the boreal landscape. This was achieved by exploring the impacts of environmental and climate factors on snow cover variability and analyzing the role of snow cover in boreal hydrology (Fig. 1).

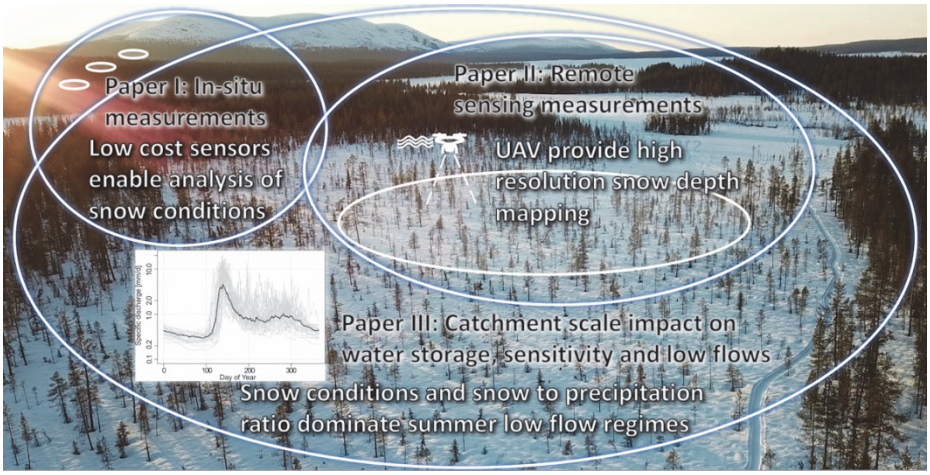


**Fig. 1. Conceptual high-level picture summarizing the scope and work performed for this thesis.**

The specific objectives were to:

1. Develop and test new robust and cost-effective measurement methods to quantify snow cover variability, using low-cost temperature loggers and unmanned aerial systems in the boreal landscape under harsh weather conditions. The key research questions in Papers I and II were: i) Can the snowpack temperature data from low-cost temperature loggers be used to determine snowmelt rates and their variability? ii) Can the UAS-SfM technique be used to map the spatial snow cover variability at a high resolution throughout the snow season in demanding weather and light conditions?
2. Analyze the snow processes in boreal conditions by utilizing the acquired data sets. This was done to investigate how different boreal landscape elements affect snow accumulation and melt patterns. The key research questions in Papers I and II were: i) What drivers are affecting local-scale spatiotemporal variations in ablation in a forest-mire hillslope? ii) How do snow accumulation, redistribution, and melt differ in forested and open landscapes?
3. Investigate the role of climate, snow, catchment characteristics, and their relative impact on catchment storage properties and low flow, to identify catchment properties that can mitigate the catchment response to climate and environmental change. The study was done by using the existing long-term and spatially well-represented time series measured from the Finnish small basin research network. The key research questions in Paper III were: i) What is the

spatiotemporal variability in storage properties and low flows in boreal catchments? ii) How the climate and catchment elements control the storage and low flows in the boreal landscape?

# 2 Study sites

This study consisted of field studies and the use of already available data. The field measurements for developing snow measurement techniques and snow process analysis (Papers I and II) were conducted at and next to the subarctic Pallas-Yllästunturi National Park area (68.00° N, 24.21° E) in Northern Finland, approximately 160km north of the Arctic circle (Fig. 2). The investigations for the relationship between climate, snow, landscape, catchment storage properties, and seasonal low flow (Paper III) were conducted using data from 61 boreal headwater catchments that form the national small basins research network in Finland (Fig. 2).

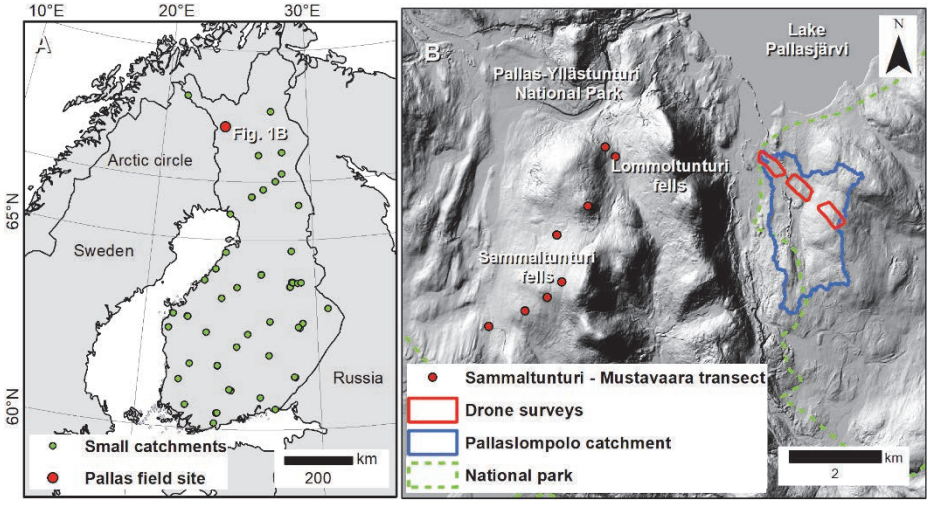


**Fig. 2. Overview of study areas, showing A) the locations of catchments in the Finnish small basin research network (see Fig. 6 for detailed illustration) and B) field plots at Pallas site. The Pallaslompolo catchment, illustrated in blue, is part of national research infrastructure in Finland, contributing to over 15 European and global research and monitoring programs (Fig. 2A data under CC BY-SA 3.0 license from Sandvik, 2009; Fig. 2B data under CC BY 4.0 license from National Land Survey of Finland, 2020).**

## 2.1 Pallas-Yllästunturi National Park field site

The field studies were carried out in two areas: Mustavaara and Sammaltunturi fells hill slope transect (Paper I), and Pallaslompolo catchment east from Lommoltunturi and Sammaltunturi fells (Paper II) (Fig. 2). These areas will be referred to as

Sammaltunturi and Pallaslompolo, respectively. The distance between areas is 5 km on average. In both areas, the landcover in the region consists mostly of boreal coniferous forests and open peatlands, but the upper slopes in the Sammaltunturi area are treeless and contain only ground vegetation (Fig. 4). The most common tree species are Norway spruce (Picea abies (L.) H. Karst) with occasional Scots pine (Pinus sylvestris L.), downy birch (Betula pubescens Ehrh.), and mountain birch (Betula pubescens ssp. czerepanovii) (Sutinen et al., 2012). In the open peatlands and in the forested areas, there are occasional bushes and other low vegetation.

The Köppen-Geiger climate classification system places the region in class Dfc, a cold climate without a dry season and with cold summers (Peel et al., 2007). The mean annual temperature in the region from 1981 to 2010 ranged between −2 °C and −1 °C and the mean annual precipitation was between 500 mm and 550 mm, based on the meteorological grid (10 $km^2$) dataset for the whole of Finland (Pirinen et al., 2012). The monthly average temperature between 1981–2010 was at the lowest in January (−13.7 °C) and highest in July (13.6 °C), calculated from the meteorological 10 $km^2$ grid dataset from the Finnish Meteorological Institute, 2021 (Fig. 3). The average snow depth on 31$^{st}$ March in the period of 1981–2010 was 60–80 cm and the average number of days with snow was 205–225 (Finnish Meteorological Institute, 2020).

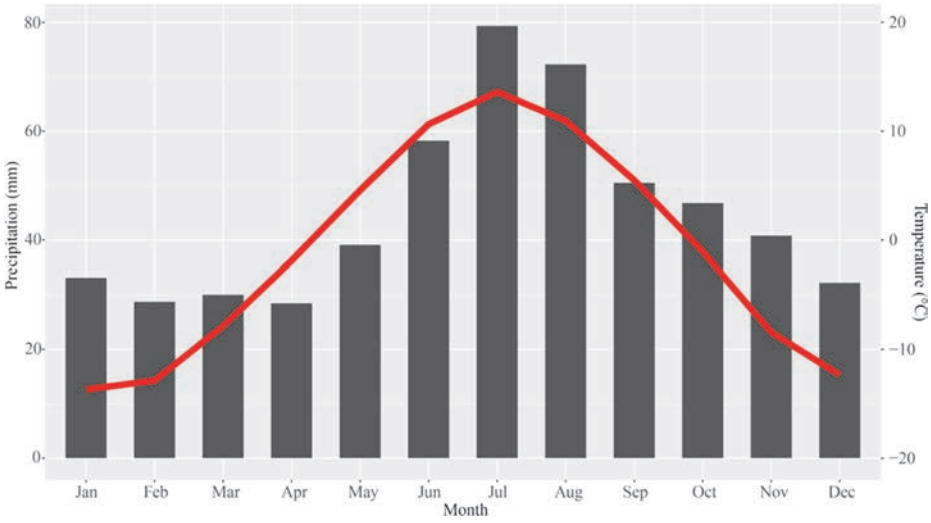


**Fig. 3. The monthly average temperature and precipitation at the Pallas area between 1981–2010, calculated from the meteorological grid (10 km$^2$) (Figure data under CC BY 4.0 license from Finnish Meteorological Institute, 2021).**

### *2.1.1 Mustavaara and Sammaltunturi field site (Paper I)*

In total, eight different experiment plots with varying topography and vegetation were established at the Sammaltunturi site in the winters of 2013/2014 and 2014/2015 (Fig. 4 and Table 1). The plots were located at the open mires (OM1 – OM3), spruce forest (SF1, SF2), forest line (FL1), transition zone on the slope (TZ1), and next to bare fell (TZ2) (Fig. 5). The elevation of the test plots varied between 320 masl and 480 masl.

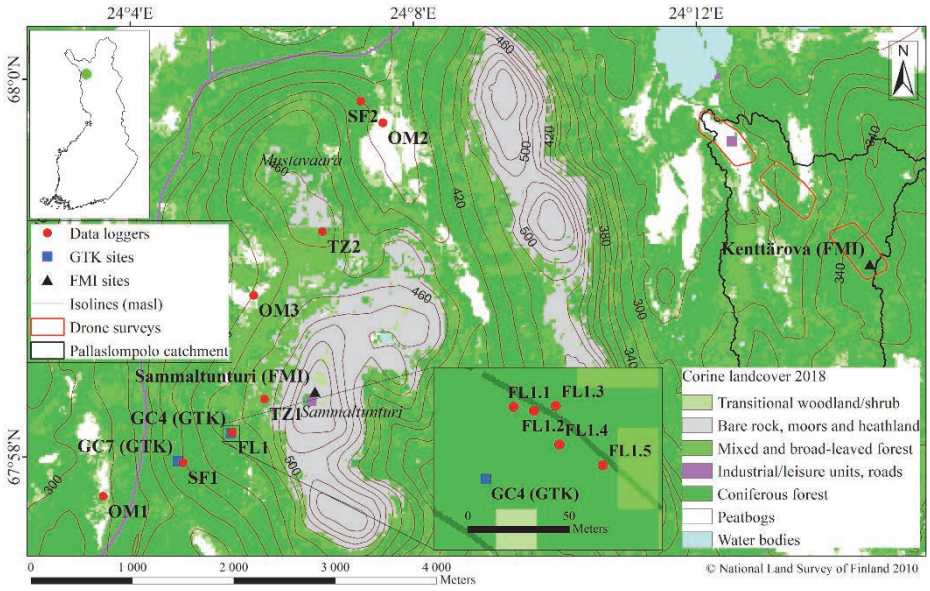


**Fig. 4. The study area and location of experiment plots, Geological Survey of Finland (GTK) acoustic snow reference measurements, and Finnish Meteorological Institute (FMI) weather stations. The area of the forest line (FL1) test plot is expanded at the center bottom (Adapted, with permission, from Paper I © 2018 Elsevier B.V.; Figure data under CC BY 4.0 license from National Land Survey of Finland, 2020 and Finnish Environment Institute, 2020).**

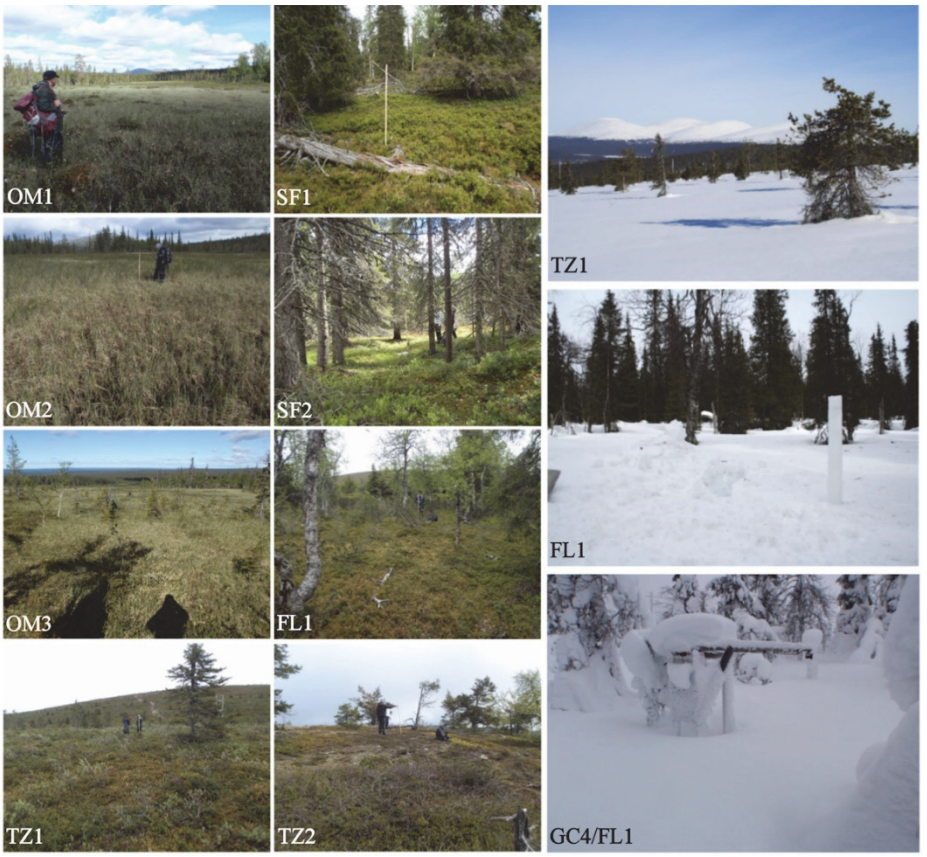


**Fig. 5. Test plots at Sammaltunturi and Mustavaara at logger collection time in summer: Open mires (OM1-OM3), spruce forest (SF1, SF2), forest line (FL1), transition zone on the slope (TZ1), and next to bare fell (TZ2). Winter pictures from TZ1 and FL1 in winter 2013/2014 and GC4/FL1 in winter 2014/2015 were taken at the time of logger installation (Reprinted, with permission, from Paper I © 2018 Elsevier B.V.).**

**Table 1. Topographical and vegetation details for measurements and reference sites. The aspect factor was calculated from slope aspect in degrees (Reprinted, with permission, from Paper I © 2018 Elsevier B.V.).**

| Site | Vegetation | Elevation (m a.s.l)[3] | Inclination (degrees)[3] | Aspect (degrees)[3] | Aspect factor[1] | Canopy coverage (%) |
|---|---|---|---|---|---|---|
| OM1 | Open mire (flat fen) | 320 | 1 | 270 | 4 | 0 |
| OM2 | Open mire (flat fen) | 375 | 1 | 70 | 5 | 0 |
| OM3 | Open mire (sloping fen) | 420 | 5 | 290 | 4 | 0 |
| SF1/GC7 | Spruce forest | 400 | 5 | 240 | 2 | 17.1 |
| SF2 | Spruce forest | 380 | 6 | 45 | 7 | 21.6 |
| FL1/GC4 | Forest line | 450 | 5 | 220 | 2 | 6.2 |
| TZ1[2] | Open slope (transitional woodland/shrub) | 475 | 4 | 270 | 4 | 0 |
| TZ2[2] | Tree line (next to bare fell | 480 | 5 | 170 | 1 | 5.1 |

[1] 1 = south, 2 = southwest, 3 = southeast, 4 = west, 5 = east, 6 = northwest, 7 = northeast, 8 = north

[2] TZ = transitional zone

[3] Topography data was extracted from a 10 m digital elevation model (National Land Survey of Finland, 2013).

### *2.1.2 Pallaslompolo field site (Paper II)*

Three test sites, Mire (14.41 ha), Mixed (15.40 ha), and Forest (15.87 ha), with varying landcover were selected at snow course transect in the Pallaslompolo catchment (Fig. 6). Mire consists mostly of flat open peatland, Forest of gently sloping coniferous forest and Mixed is a relatively flat mixture of the two. The elevation in the study area varies from 267 to 350 masl, the slope between 0–4.76 degrees and the overall aspect is towards the west-northwest. Peatland areas, at Mire and Mixed, are almost flat with a slope of only 0–0.25 degrees, while the slope is highest in parts of the forested area at Forest.

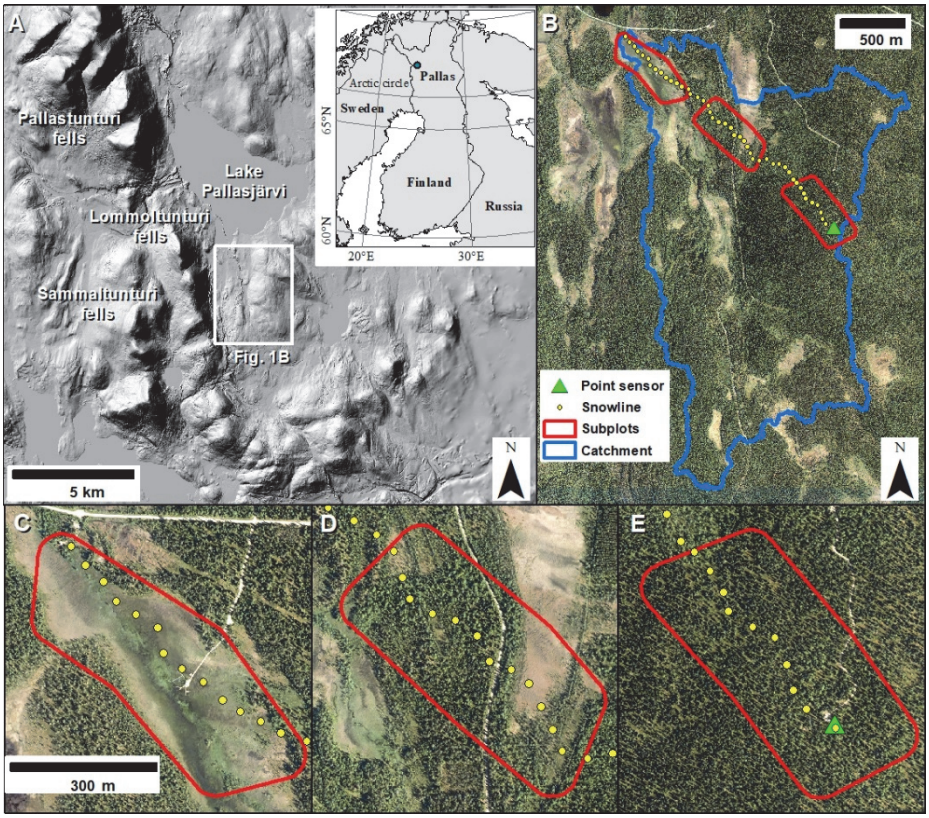


**Fig. 6. A) Location of the study site south of Lake Pallasjärvi and east of the Lommoltunturi fells. The location of Fig. 1B is highlighted by the white rectangle. B) Locations of the manual snowline measurement, ultrasonic point sensor, and outlines of the subplots (Mire, Mixed, and Forest read from northwest to southeast) within the catchment. Figs C, D, and E zoom in to subplots Mire, Mixed, and Forest, respectively (Reprinted, with permission, from Paper II © 2021 Authors; Fig. 6A data under CC BY 4.0 license from National Land Survey of Finland, 2020 and under CC BY-SA 3.0 license from Sandvik, 2009; Figs. 6B–E data under CC BY 4.0 license from National Land Survey of Finland, 2020b).**

## 2.2 Small basins research network in Finland (Paper III)

This work was conducted using data from 61 boreal headwater catchments (Fig. 7, Table 2) that form the national small basins research network in Finland (Seuna, 1983). The area of the catchments ranges from 0.07 to 79.20 km$^2$ (median 6.15

km$^2$), while the topography is relatively flat, with a mean slope ranging from 1.1° to 12.5° (median 3.1°) and mean elevation from 15 to 557 m above sea level (median 144 m above sea level). The dominant land cover type is forest (median 80% of surface area), followed by peatland (median 26%), while agricultural areas are relatively common in coastal regions in southern and southwestern Finland, where the surface geology is mainly clay and silt. Most of the surface geology in the study catchments is basal till (median 60% of catchment area). Sand/gravel and glaciofluvial deposits (hereafter referred to as "sand/gravel soil") also occur (median 0%, mean 6%). The climate in Finland is humid, with a mean annual temperature of 5 °C in the south and −2 °C in the north, the mean precipitation is 700 and 450 mm, respectively, and the mean snow depth by the end of March is 5 and 80 cm, respectively (Pirinen et al., 2012). Many climate and catchment characteristics covary from the coast to inland and from south to north. In particular, clay/silt soils and agricultural areas are positively associated with air temperature (and negatively with snow), while peatlands and till soils are negatively associated with air temperature (and positively with snow). The mean elevation also shows a negative association with air temperature, as the ground elevation increases from coastal areas to inland and from the south to the north.

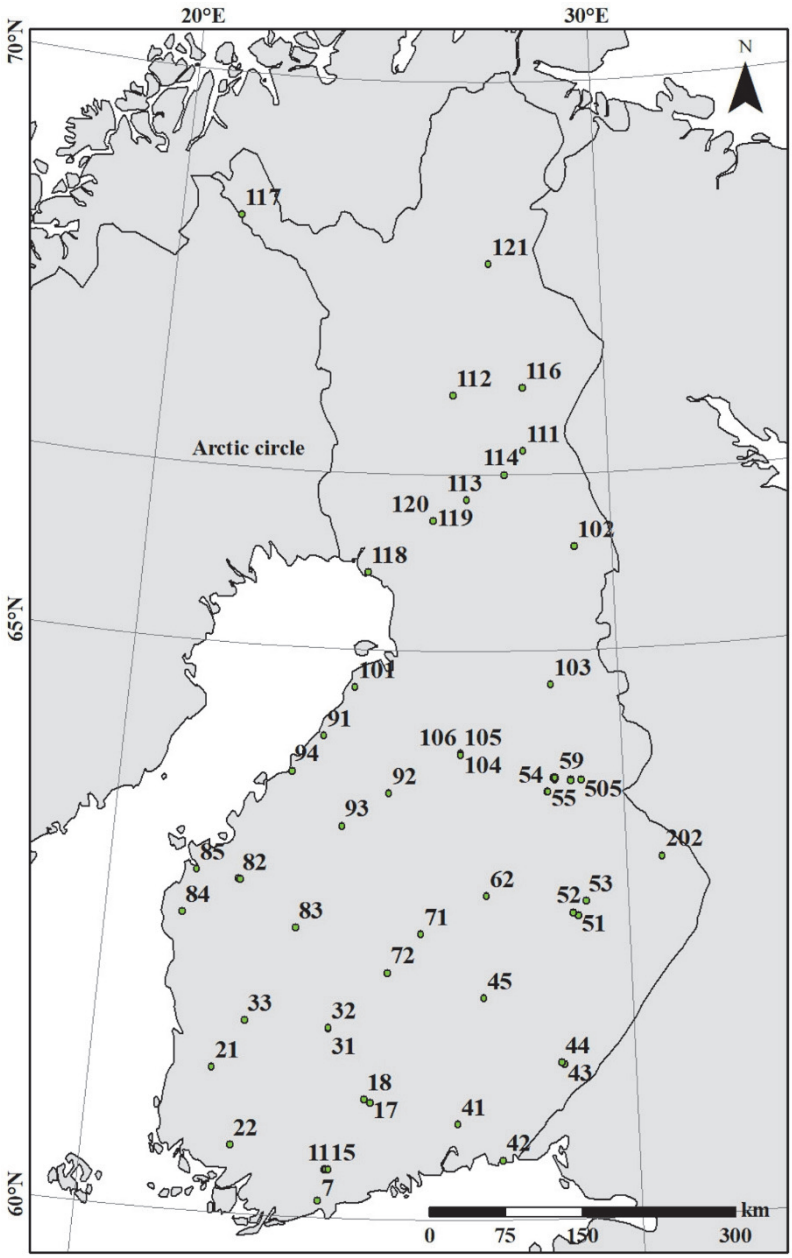


**Fig. 7. Study catchments in the Finnish small basin research network with their respective catchment ID (Figure data under CC BY-SA 3.0 license from Sandvik, 2009).**

**Table 2. The physiographical and land cover characteristics of the study catchments (Reprinted, with permission, from Supporting Information of Paper III © 2019 American Geophysical Union).**

| ID | Name | Area ($km^2$) | Basal till (%) | Sand/ Gravel (%) | Clay/ silt (%) | Peatland (%) | Drained peatland (%) | Pristine peatland (%) | Agri-culture (%) | Mean elevation (masl) | Slope (°) | Lakes (%) | Forest mineral soil (%) | Forest peatland (%) |
|---|---|---|---|---|---|---|---|---|---|---|---|---|---|---|
| 7 | Rudbäcken1 | 1.42 | 23 | 0 | 0 | 12 | 8 | 4 | 0 | 42 | 9 | 1.8 | 58 | 8 |
| 11 | Hovi | 0.12 | 0 | 0 | 60 | 0 | 0 | 0 | 97 | 49 | 2 | 0 | 0 | 0 |
| 12 | Ali-Knuuttila | 0.25 | 0 | 0 | 17 | 0 | 0 | 0 | 48 | 64 | 6 | 0 | 37 | 0 |
| 13 | Yli-Knuuttila | 0.07 | 0 | 0 | 100 | 0 | 0 | 0 | 0 | 70 | 13 | 0 | 86 | 0 |
| 14 | Teeressuonoja | 0.69 | 94 | 6 | 0 | 12 | 1 | 11 | 0 | 78 | 7 | 0 | 74 | 11 |
| 15 | Kylmänoja | 4.04 | 5 | 24 | 46 | 10 | 8 | 1 | 19 | 74 | 5 | 0 | 54 | 8 |
| 17 | Koppelonoja | 7.81 | 10 | 12 | 49 | 6 | 6 | 1 | 23 | 139 | 6 | 0 | 59 | 5 |
| 18 | Löyttynoja | 8.2 | 15 | 44 | 25 | 16 | 14 | 2 | 17 | 144 | 7 | 0 | 60 | 14 |
| 21 | Löytäneenoja | 5.64 | 14 | 3 | 83 | 3 | 2 | 1 | 63 | 41 | 2 | 0.1 | 26 | 0 |
| 22 | Savijoki | 15.4 | 0 | 0 | 60 | 3 | 3 | 1 | 39 | 63 | 4 | 0 | 46 | 1 |
| 31 | Paunulanpuro | 1.5 | 71 | 0 | 1 | 13 | 10 | 3 | 0 | 132 | 5 | 0 | 88 | 8 |
| 32 | Siukolanpuro | 1.86 | 60 | 0 | 16 | 56 | 42 | 14 | 0 | 119 | 6 | 0 | 81 | 6 |
| 33 | Katajaluoma | 11.2 | 14 | 37 | 1 | 38 | 34 | 4 | 3 | 123 | 3 | 0 | 55 | 34 |
| 41 | Niittyjoki | 29.7 | 7 | 27 | 58 | 6 | 5 | 1 | 25 | 64 | 3 | 0.1 | 43 | 1 |
| 42 | Ravijoki | 56.9 | 35 | 9 | 22 | 17 | 13 | 4 | 13 | 30 | 4 | 0.9 | 61 | 12 |
| 43 | Latosuonoja | 5.34 | 5 | 37 | 0 | 12 | 12 | 0 | 15 | 95 | 5 | 0 | 69 | 11 |
| 44 | Huhtisuonoja | 5.03 | 11 | 34 | 0 | 45 | 43 | 2 | 0 | 107 | 2 | 0 | 52 | 44 |
| 45 | Juonistonoja | 13 | 84 | 0 | 0 | 23 | 22 | 1 | 11 | 129 | 1 | 0 | 64 | 18 |
| 51 | Kesselinpuro | 21.7 | 75 | 0 | 0 | 36 | 34 | 2 | 1 | 116 | 3 | 0.8 | 61 | 33 |
| 52 | Kuokkalanoja | 2.67 | 100 | 0 | 0 | 9 | 9 | 1 | 5 | 122 | 4 | 0 | 74 | 8 |
| 53 | Mustapuro | 11.2 | 43 | 23 | 7 | 35 | 32 | 2 | 8 | 97 | 3 | 0.1 | 54 | 32 |
| 54 | Murtopuro | 4.94 | 100 | 0 | 0 | 54 | 44 | 10 | 0 | 214 | 3 | 0 | 69 | 25 |

| ID | Name | Area ($km^2$) | Basal till (%) | Sand/ Gravel (%) | Clay/ silt (%) | Peatland (%) | Drained peatland (%) | Pristine peatland (%) | Agri-culture (%) | Mean elevation (masl) | Slope (°) | Lakes (%) | Forest mineral soil (%) | Forest peatland (%) |
|---|---|---|---|---|---|---|---|---|---|---|---|---|---|---|
| 55 | Liuhapuro | 1.65 | 77 | 0 | 0 | 55 | 23 | 31 | 0 | 213 | 3 | 0 | 59 | 37 |
| 56 | Suopuro | 1.13 | 40 | 0 | 0 | 68 | 23 | 45 | 0 | 210 | 2 | 0 | 34 | 30 |
| 57 | Välipuro | 0.86 | 100 | 0 | 0 | 55 | 15 | 40 | 0 | 199 | 3 | 0 | 39 | 43 |
| 58 | Kivipuro | 0.54 | 78 | 0 | 0 | 32 | 12 | 20 | 0 | 199 | 3 | 0 | 71 | 29 |
| 59 | Koivupuro | 1.18 | 68 | 0 | 0 | 53 | 33 | 19 | 0 | 219 | 3 | 0 | 37 | 44 |
| 62 | Kohisevanpuro | 10.65 | 79 | 0 | 0 | 26 | 22 | 4 | 1 | 148 | 4 | 0.2 | 68 | 20 |
| 71 | Ruunapuro | 5.39 | 68 | 17 | 5 | 13 | 12 | 2 | 17 | 132 | 4 | 0 | 65 | 11 |
| 72 | Heinäjoki | 9.4 | 96 | 0 | 0 | 16 | 14 | 2 | 3 | 167 | 6 | 0.1 | 76 | 11 |
| 81 | Haapajyrä | 6.09 | 9 | 0 | 51 | 12 | 11 | 0 | 55 | 32 | 3 | 0 | 24 | 11 |
| 82 | Kainastonluoma | 79.2 | 46 | 1 | 22 | 20 | 18 | 3 | 24 | 43 | 3 | 0.2 | 48 | 15 |
| 83 | Kaidesluoma | 45.5 | 57 | 0 | 4 | 31 | 26 | 2 | 10 | 145 | 2 | 1.2 | 51 | 20 |
| 84 | Norrskogsdiket | 11.6 | 48 | 0 | 34 | 22 | 9 | 13 | 34 | 29 | 2 | 0.1 | 40 | 8 |
| 85 | Sulvanjoki | 26.85 | 78 | 0 | 20 | 11 | 10 | 1 | 20 | 20 | 3 | 0 | 65 | 8 |
| 91 | Tuuraoja | 23.5 | 24 | 19 | 13 | 44 | 35 | 9 | 23 | 39 | 2 | 0 | 32 | 30 |
| 92 | Tujuoja | 20.5 | 67 | 0 | 23 | 32 | 32 | 1 | 5 | 124 | 2 | 0 | 58 | 24 |
| 93 | Pahkaoja | 23.3 | 65 | 5 | 0 | 46 | 31 | 16 | 2 | 177 | 2 | 0.9 | 46 | 24 |
| 94 | Kuikkisenoja | 8.05 | 67 | 0 | 16 | 16 | 13 | 3 | 25 | 15 | 3 | 0.2 | 52 | 14 |
| 101 | Huopakinoja | 19.7 | 62 | 17 | 17 | 28 | 26 | 3 | 14 | 37 | 2 | 0 | 57 | 21 |
| 102 | Vääräjoki | 19.3 | 95 | 1 | 0 | 43 | 8 | 35 | 0 | 301 | 4 | 0.8 | 53 | 19 |
| 103 | Myllypuro | 9.86 | 69 | 0 | 0 | 32 | 27 | 5 | 0 | 210 | 4 | 0.5 | 66 | 25 |
| 104 | Murronoja | 4.38 | 42 | 0 | 0 | 69 | 59 | 10 | 0 | 181 | 2 | 0 | 38 | 55 |
| 105 | Koppamäenoja | 6.15 | 64 | 0 | 0 | 56 | 32 | 25 | 0 | 190 | 3 | 0.7 | 41 | 41 |
| 106 | Kaukolanpuro | 4.84 | 56 | 0 | 0 | 52 | 49 | 2 | 0 | 190 | 2 | 0 | 45 | 46 |
| 111 | Kuusivaaranpuro | 27.6 | 64 | 0 | 0 | 36 | 29 | 7 | 0 | 236 | 2 | 0 | 62 | 27 |
| 112 | Lismanoja | 2.77 | 14 | 0 | 0 | 42 | 17 | 8 | 0 | 234 | 3 | 0 | 46 | 9 |

| ID | Name | Area ($km^2$) | Basal till (%) | Sand/ Gravel (%) | Clay/ silt (%) | Peatland (%) | Drained peatland (%) | Pristine peatland (%) | Agri-culture (%) | Mean elevation (masl) | Slope (°) | Lakes (%) | Forest mineral soil (%) | Forest peatland (%) |
|---|---|---|---|---|---|---|---|---|---|---|---|---|---|---|
| 113 | Korintteenoja | 6.13 | 57 | 0 | 0 | 12 | 5 | 7 | 3 | 216 | 7 | 0.5 | 81 | 8 |
| 114 | Vähä-Askanjoki | 16.4 | 100 | 0 | 0 | 26 | 6 | 21 | 0 | 278 | 6 | 0.1 | 76 | 12 |
| 116 | Myllyoja | 28.5 | 50 | 4 | 0 | 18 | 8 | 10 | 0 | 252 | 5 | 0 | 69 | 8 |
| 117 | Iittovuoma | 11.6 | 60 | 0 | 0 | 12 | 0 | 12 | 0 | 557 | 7 | 1.3 | 17 | 0 |
| 118 | Kirnuoja | 6.79 | 51 | 0 | 0 | 35 | 14 | 21 | 0 | 17 | 2 | 0.4 | 60 | 18 |
| 119 | Ylijoki | 56.27 | 66 | 1 | 0 | 55 | 36 | 19 | 1 | 185 | 2 | 2.1 | 41 | 31 |
| 120 | Kotioja | 18.11 | 57 | 0 | 0 | 49 | 31 | 18 | 1 | 189 | 2 | 0.2 | 51 | 28 |
| 121 | Laanioja | 13.62 | 27 | 19 | 0 | 5 | 0 | 5 | 0 | 328 | 5 | 0.1 | 66 | 0 |
| 202 | Pieni Hietajärvi | 0.67 | 70 | 0 | 0 | 47 | 2 | 45 | 0 | 170 | 3 | 4.6 | 49 | 21 |
| 501 | Kauheanpuro | 1.76 | 66 | 0 | 0 | 51 | 18 | 33 | 0 | 209 | 3 | 2.5 | 47 | 32 |
| 502 | Korsukorvenpuro | 0.72 | 47 | 0 | 0 | 53 | 7 | 47 | 0 | 210 | 2 | 0 | 44 | 29 |
| 503 | Kangasvaaranpuro | 0.56 | 100 | 0 | 0 | 9 | 3 | 6 | 0 | 214 | 7 | 0 | 93 | 5 |
| 504 | Kangaslammenpuro | 0.3 | 100 | 0 | 0 | 10 | 3 | 6 | 0 | 213 | 7 | 0 | 90 | 10 |
| 505 | Porkkasalonpuro | 0.72 | 100 | 0 | 0 | 18 | 12 | 6 | 0 | 203 | 6 | 0 | 80 | 17 |

# 3 Materials and methods

## 3.1 Field methods to monitor snow variability

The observations of snow cover variability were conducted using in-situ (Paper I) and remote sensing (Paper II) methods. For in-situ observations, low-cost temperature loggers were placed in the snowpack in varying topography and vegetation conditions, and the temperature data variability from the loggers was used to determine snow cover disappearance and snowmelt progress in late winter. For remote sensing, UAS platform and SfM techniques were used to determine the snow depth in high-resolution, covering a mosaic of different land cover and vegetation patterns. The in-situ measurements focused on the snowmelt period for two separate years, whereas the remotely sensed measurements covered the whole snow season, from accumulation to melt.

### *3.1.1 In-situ: Temperature loggers (Paper I)*

At each plot, the temperature sensors were placed at five points and two heights in the snowpack: on the ground and at a fixed height of 30 cm above the ground. The distance between the test points was approximately 10–50 m, which can be defined as microscale. The distance between test plots was approximately 500–4000 m, which is considered a local (meso) scale (Don M. Gray, 1978; Kuusisto, 1984; Rasmus, 2005). Waterproof Onset Hobo Pedant model UA-001-08 temperature data loggers were used to record the snow temperature. For the first winter, the temperature logging with 15-min recording intervals started on 19$^{th}$ April and ended on 16$^{th}$ June, whereas, for the second winter, the temperature was recorded using 30-min intervals from 28$^{th}$ February to 27$^{th}$ June.

Daily data from acoustic snow depth sensors (SR50A, Campell Scientific) at measurement stations GC7 and GC4 (Fig. 3, Fig. 4 GC4/FL1), adjacent to the SF1 and FL1 test plots, was used as a reference for the temperature logger-based results. Reference data was not available after 25$^{th}$ May in spring 2015. The water content of the soil was measured at the reference stations using CS615 TDR (time-domain reflectometer) probes installed 20 cm below ground (Sutinen et al., 2008, 2009). These were used to validate the snowmelt simulations with an empirical snow model (more information in Paper I).

The changes in diurnal temperature variation were used as the criterion to determine if the logger was free of snow (Fujihara et al., 2017; Reusser & Zehe, 2011). 2.0 °C for the standard deviation of the diurnal sensor temperature values was used as the threshold for the detection. When the criterion was satisfied, it was assumed for that day that the snow depth was equal to the logger height from the ground. This method is based on the strong insulation properties of snow, which decrease the temperature variations. In its current form, the method detects the first date when the criteria are fulfilled. This method can have issues detecting the correct date in cases of oscillation of the snow depth above and below the logger position, but this was not the case during our study period. More information on the algorithm can be found in Paper I.

Commonly used degree-day factors (ddf) for each point were calculated using the equation

$$\mathrm{ddf} = \frac{(h_{0.3} - h_0) \times \frac{\rho_S}{\rho_W}}{t_m \times (T_a - T_m)}, \quad (1)$$

where $h_{0.3}$ is the snowpack thickness (0.3 m) when the upper logger is exposed from the snowpack and $h_0$ is the ground level which is determined when the logger on the ground is exposed. Density of snow $\rho_s$ is assumed to be 329 kg m$^{-3}$ in forested areas and 349 kg m$^{-3}$ in open areas (Kuusisto, 1984), and water density $\rho_w$ is assumed to be 1000 kg m$^{-3}$. Time for the melt between $h_{0.3}$ and $h_0$ is marked with $t_m$, while $T_a$ is the mean air temperature during the melt and $T_m$ is the threshold for snowmelt, assumed to be 0 °C. The calculated degree-day factors are averaged for the final 0.3 m period of snowmelt, assuming minimal snow density changes. The determined degree-day factors were successfully applied in an empirical snow model. For more information, the reader is referred to Paper I.

### *3.1.2 Remote sensing: Drones (Paper II)*

Three different quadcopters (DJI Mavic Pro, DJI Phantom 4 Advanced, and DJI Phantom 4 Real-Time Kinematic (P4RTK) and a fixed-wing drone (SenseFly eBee Plus RTK) were utilized to map the test sites in the Pallaslompolo area (Table 3). The drones were selected because of their different properties in terms of portability, camera, flight time, and positioning accuracy.

**Table 3. Drone properties (Adapted, with permission, from Rauhala et al., 2021 © 2021 Authors).**

| UAS | Mavic Pro[3] | Phantom 4 Adv.[4] | Phantom 4 RTK[5] | eBee Plus RTK[6] |
|---|---|---|---|---|
| Portability[1,7] | High | Average | Average | Low |
| Flight time (min) | 27 | 30 | 30 | 59 |
| Max. speed (km/h) | 65 | 72 | 72 | 110 |
| Sensor size (inch) | 1/2.3" | 1" | 1" | 1" |
| Effective megapixels | 12.4 | 20 | 20 | 20 |
| Focal length (mm, 35 mm equiv.) | 26 | 24 | 24 | 29 |
| Field of view (°) | 79 | 84 | 84 | 64 |
| Ground resolution at 100 m (cm/pixel)[7] | 3.1 | 2.7 | 2.7 | 2.3 |
| Take-off/landing area[2,7] | Small | Small | Small | Large |

[1] High = shoulder bag, Average = special backpack, Low = 75x48x33 cm case

[2] Small = vertical take-off and landing (approx. < 5x5m open area), Large = runway like open space (approx. > half of a soccer field)

[3] Data source: https://www.dji.com/fi/mavic/info.

[4] Data source: https://www.dji.com/fi/phantom-4-adv/info#specs

[5] Data source: https://www.dji.com/fi/phantom-4-rtk/info#specs

[6] Data source: eBee+ brochure (not available in web), [7] Defined and calculated by Authors

The drones with internal GPS correction (RTK) have a remarkable advantage over the others in terms of field workload. They only need one external ground control point (GCP), while the drones without RTK need several external GCP spread around the study area (at a distance of approximately 50 m in between), where the location measured using RTK GNSS receiver, to rectify the aerial images. Trimble R10 and Topcon Hiper-V RTK GNSS receivers were used to measure GCPs in this study.

Data from five of the seven UAS campaigns was selected for the snow process analysis (Table 4). Two of the surveys were discarded due to challenges during the campaigns that hindered the data collection from all study plots. During the snow period, the remaining surveys were conducted in varying snow, weather, and light conditions, at the beginning (DEC-12) and middle (FEB-21) of the snow accumulation period, one at the beginning of the melt period (APR-03, shortly after peak accumulation) and one in the middle of the melt period (APR-24). The last survey (4–5$^{th}$ June 2019), for the snow snow-free conditions, was conducted before ground vegetation growing season (when the vegetation was still compressed), approximately one week after all snow had melted. The data from P4RTK was

selected for snow process analysis because it provided the highest accuracy for snow and ground surface maps created using the SfM photogrammetry technique (Rauhala et al., 2021).

**Table 4. UAS survey times (Adapted, with permission, from Rauhala et al., 2021 © 2021 Authors).**

| UAS campaign | Mavic Pro | Phantom 4 Adv. | Phantom 4 RTK | eBee Plus RTK |
|---|---|---|---|---|
| 10–13.12.2018 | X | X | X | X |
| 21–25.01.2019 | x[1] | | | |
| 18–22.02.2019 | X | | X | X |
| 01–05.04.2019 | X | | X | X |
| 22–25.04.2019 | X | | X | |
| 20–21.05.2019 | x[1] | x[1] | | |
| 04–05.06.2019 | | | X | X |

[1] discarded due to challenges in data collection

The principal technique for snow depth map generation was subtracting snow surface elevations from snow snow-free ground elevations. Agisoft Metashape/Metashape Professional v1.4.5./v.1.6 software utilizing the SfM technique (Westoby et al., 2012) was used to create surface elevation maps using high quality and moderate depth filtering settings. This resulted in full resolution (~3 cm) orthomosaic and ~7 cm resolution snow and ground surface maps or digital surface models (DSMs). The processed data was exported as georeferenced files to ESRI ArcGIS 10.6 for further processing.

Due to poor sub-canopy penetration using the UAS-SfM method (Harder et al., 2020), data at tree locations, and immediately next to trees, was omitted using special tree masks. Tree masks were generated using Maximum Likelihood Supervised Classification in ESRI ArcGIS 10.6 and full-resolution orthomosaics from the survey conducted on 3rd April, 2019. This survey was selected because snow had melted from tree canopies, creating a high contrast between trees and snow, which was used for classifying the data. The SfM method had challenges in differentiating between trees and snow cover during the surveys when the canopies were covered by snow, leading to artificially increased snow depths next to the tree branches. Moreover, the deciduous trees without leaves were problematic in supervised classification because bare branches were easily mixed with shadowed snow cover, leading to shadowed snow cover being classified as canopy or canopy as snow cover. To mitigate these methodological challenges, different buffer distances around the classified tree mask were tested and 36 cm was found to be a

good compromise to remove the problematic zones next to trees without losing too much valuable snow cover data. After buffering, the tree masks were saved with a resolution of 2 cm and applied to snow and ground surface maps before snow depth calculation.

Snow depths were calculated for each pixel by subtracting bare ground (snow-free) elevation from snow surface elevation for each survey done in snow season, resulting in DEM of differences (DoDs). Snow depth maps were aggregated to 50 cm resolution before further data analysis. This resolution was chosen to smooth small-scale variability while keeping a reasonably high resolution for snow-vegetation interaction analysis. Moreover, the standard deviation of snow depth has been observed to increase with decreased pixel size but stabilize at resolutions smaller than 1 m (De Michele et al., 2016). To analyze snow depth variability compared to point measurement, anomaly maps were created by subtracting corresponding snow depth measured with ultrasonic sensor from each pixel of the UAS-SfM derived snow depth maps. This snow depth from the ultrasonic sensor was also subtracted from reference snow course measurements.

Corine land cover 2018 data with a resolution of 20 m (Finnish Environment Institute, 2020) was further used to study the snow processes for different landcover types: coniferous forest (10.07 ha), mixed forest (1.42 ha, combined from mixed (1.34 ha) and broadleaved forest (0.08 ha) land cover types), transitional woodland/shrub (1.06 ha) and peatbogs (10.37 ha) (Fig. 8). The Corine land cover dataset was selected for this purpose due to its i) approved vegetation classification and ii) availability across the Eurasian region. To further study the interactions between canopy cover and snow depth, the Euclidian distance from the nearest tree mask pixel, representing the canopy, was calculated for each snow pixel in ESRI ArcGIS 10.6 (Fig. 8). These distance masks were used to calculate the median snow depth as a function of distance from the canopy for each land cover type.

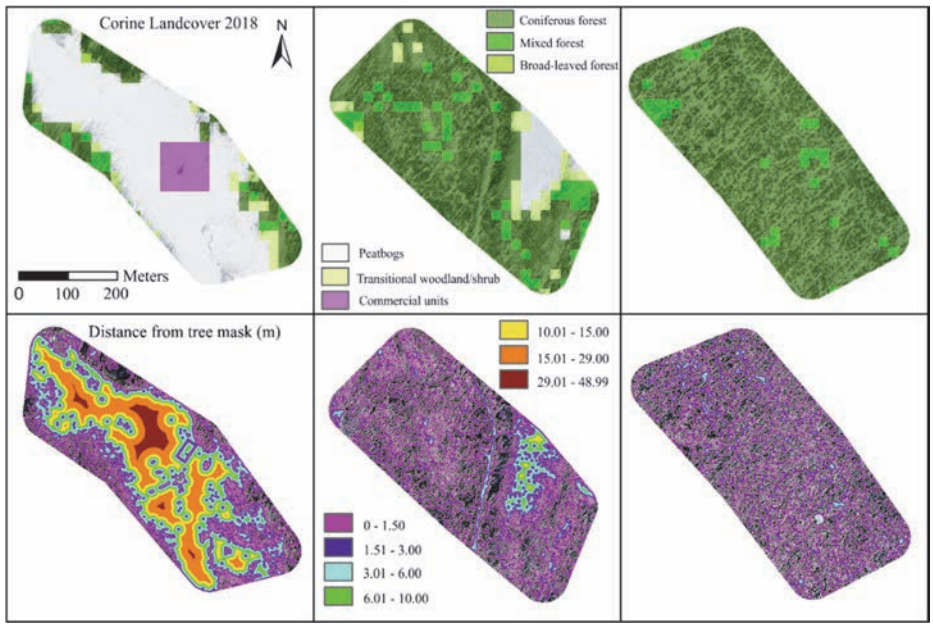


**Fig. 8. Corine land cover (2018) data and distance from tree mask (calculated using Euclidian distance tool in ESRI ArcGIS 10.6) for test sites. "Commercial units" refers to measurement infrastructure in the peatbog (Reprinted, with permission, from Paper II © 2021 Authors; Figure data from Paper II and under CC BY 4.0 license from Finnish Environment Institute, 2020).**

## 3.2 Catchment scale relationships between catchment storage, low-flows and catchment characteristics (Paper III)

Two approaches for recession analysis were used to calculate the catchment water storage ($S_C$) and storage sensitivity of streamflow ($\varepsilon_S$). Both approaches are based on the same method and on the assumption that terrestrial water storage is the only source of streamflow (Brutsaert & Nieber, 1977). Because of this assumption and to avoid the impacts of evapotranspiration and snowmelt (Kirchner, 2009), the recession periods were analyzed for September – December. Furthermore, days with more than 0.9 mm of precipitation were discarded from the analysis, and the minimum recession length was set to 7 days and removed the first 3 days of the recession, a procedure adapted from (Berghuijs et al., 2016), to minimize the effect of precipitation and fast runoff processes. Lumped analysis for the recession periods was used in place of individual recessions.

The recession rate *dQ/dt* and daily streamflow *Q* reveal an approximately linear association when plotted in the log-log scale, suggesting a power-law relationship

$$\frac{dQ}{dt} = -\alpha Q^{\beta}, \tag{2}$$

where $\alpha$ and $\beta$ can be derived using linear regression. In the first approach, by assuming linear reservoir model ($\beta$ = 1) and the linear storage-discharge relationship between annual catchment storage and annual maximum baseflow, the catchment water storage $S_C$ (mm) was further calculated by equation

$$S_C = KQ_{Max\_BF}, \tag{3}$$

where *K* is the recession constant 1/$\alpha$ (Arciniega-Esparza et al., 2017; Brutsaert, 2008).

The second approach utilized the storage sensitivity of streamflow $\varepsilon_S$ (1/mm), introduced by (Berghuijs et al., 2016), which is defined as a change in normalized streamflow *dQ/Q* divided by the change in catchment storage *dS* in the form

$$\varepsilon_S = \frac{dQ/Q}{dS}. \tag{4}$$

This can be further expressed as

$$\varepsilon_S(\alpha, \beta, Q) = \alpha Q^{\beta-2}, \tag{5}$$

where *Q* is the flow rate of interest. $Q_{85}$ flow was used to calculate the storage sensitivity of streamflow for low flow conditions, as in (Berghuijs et al., 2016). In addition to $\alpha$, parameter $\beta$ was determined using recession analysis, allowing for nonlinear catchment storage–discharge relationships (equation (2)). Because $\beta$ is determined from the recession, parameter $\alpha$ is also different from the catchment storage calculations. For more information about the method, the reader is referred to Paper III.

From the daily data sets, the median of annual values was calculated for specific discharge (Q), precipitation (P), temperature (T), potential evapotranspiration (PET), maximum snow water equivalent (max SWE), day of the year for max SWE, and end of the snow cover. Seven-day low flow indices were calculated separately for winter (February–March) and summer (July–August) from daily streamflow records for each catchment. The selected months cover the typical timing of low flow conditions during winter due to sub-zero temperatures and during summer due to high evapotranspiration.

The sensitivity of streamflow to climate was calculated using climate elasticity to precipitation with the contribution of evaporation (Sun et al., 2013) as

$$\varepsilon_P = \text{median}\left(\frac{\Delta Q/\overline{Q} - \Delta PET/\overline{PET}}{\Delta P/\overline{P} - \Delta PET/\overline{PET}}\right), \quad (6)$$

where $\varepsilon_P$ is climate elasticity (dimensionless), Q (mm/year) is annual streamflow, PET (mm/year) is annual potential evaporation, and the superscript line denotes long-term average. Class A pan-measurement data from the Finnish Environment Institute was used to calculate the annual sum of PET. The dimensionless wetness index P/PET was taken as the median of its annual values. The annual median snow fraction (dimensionless) of total precipitation, i.e. snow to precipitation (S/P) ratio, was calculated using 1.1°C as the threshold for snowfall (Feiccabrino & Lundberg, 2008; Lendzioch et al., 2016).

A multivariant principal component analysis (PCA) was performed to study the relationships between catchment characteristics and climate indices because many of them showed strong collinearity, and to reduce the number of variables and delineate patterns from the data (for more information, see Paper III). The scores from significant principal components (PC) were then used to study their relationship to catchment storage, storage sensitivity, and low flows, using Generalized Additive Models (GAMs), which are extensions of generalized linear models (Hastie & Tibshirani, 1990). The GAM analysis was used to find possible nonlinear relationships, as the runoff-generating processes are often nonlinear. In a semiparametric GAM, the linear predictor variable is substituted with an unspecified smooth function estimated using a scatterplot smoother by equation

$$g(\mu) = \alpha + \sum_{j=1}^{p} f_j(x_j), \quad (7)$$

where $g$ is the link function, $\mu$ is the expected value of the response variable related to predictor variable $x$, $\alpha$ is a constant, and $f$ is the unspecified smooth functions. The degrees of freedom in fitted models were allowed to vary between 1 (linear relationship) and 3 (nonlinear relationship) to avoid model overfitting. The quality of GAMs was analyzed using leave-one-out cross-validation (LOOCV) by plotting the response curve shapes to the same graphs as the original models (Hastie et al., 2001) and comparing the range of $p$-values and explained deviances between original models and the LOOCV results.

# 4 Results

## 4.1 Low-cost temperature sensors enable analysis of snow conditions (Paper I)

### *4.1.1 Timing and variability of snowmelt*

The detected timing of snowmelt using temperature data with the developed algorithm agreed reasonably well with snow depth data from the adjacent reference station (Fig. 9). The data from temperature sensors showed no fluctuation while the sensors were located under the insulating snow cover and started to follow the air temperature when exposed. These detection timings from test points enabled further study of the variability of snowmelt between and within test plots.

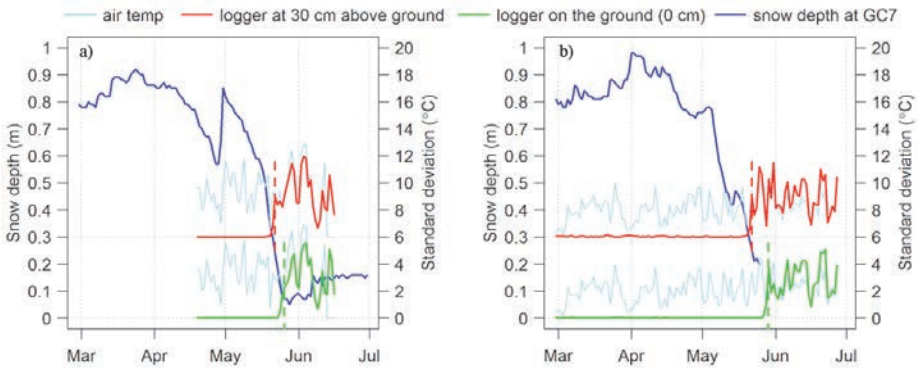


**Fig. 9. Daily standard deviation in logger temperatures and snow depth in reference measurement station. Reference measurements were assumed to be disturbed by the movement of the supporting structure showing small fluctuations in the snow depth, and the underbrush, which prevented the snow depth from reaching zero cm. Logger temperature data at a height of 30 cm has been offset to 30 cm snow depth to visualise the logger position in the snowpack (Reprinted, with permission, from Paper I © 2018 Elsevier B.V.).**

Generally, open mires (OM1, OM2, and OM3) and plots where the canopy cover was very low (TZ2) or non-existing (TZ1) showed earlier snowmelt (Fig. 10). In contrast, the north-facing forested slope (SF2) showed the latest snowmelt, while

in the forested south-western slope (SF1) the melt occurred in between the open areas and north-facing forest.

An annual comparison using data from test plots SF1, SF2, FL1, and OM2, in which measurements were done during both study winters, showed similar snow cover depletion timings. The average date for snow depletion was 27th May (range 10 days, 23 May–2 June) in 2014 and 28th May (range 8 days, 24 May–1 June) in 2015. The variation in snow cover depletion was lowest in the open mire and highest in the forested sites in 2014, while inconsistent trends were found in 2015. The observed overall variability of snow depletion timing was higher than the variability within a plot.

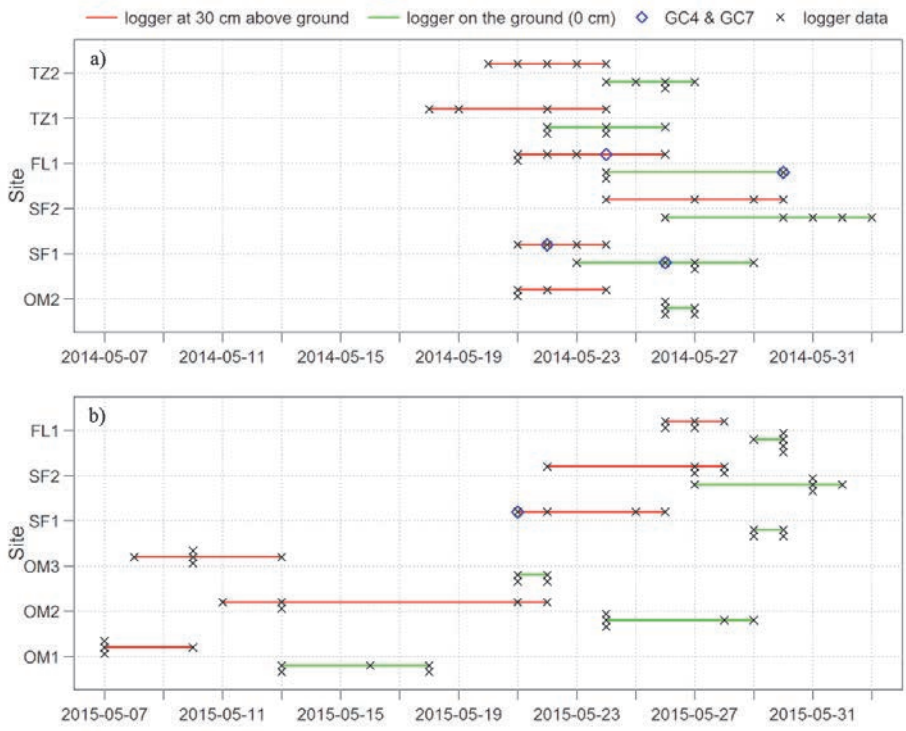


**Fig. 10. The observed variability in snow cover depletion in 2014 and 2015, derived using logger temperatures (Reprinted, with permission, from Paper I © 2018 Elsevier B.V.).**

### *4.1.2 Melt rates and degree-day factors*

Degree-day factors determined for each test point showed notably within the year and interannual variation (Table 5, Fig. 11). The highest median ddf values were found in the highest elevation test plots (TZ1, TZ2 in 2014, and FL1 in 2015) on the south-facing slope. The median ddf value obtained for the open mire (OM2) in 2014 was higher than in forested plots (SF2, FL1), but lower than in open transitional slope plots (TZ1, TZ2) and the southwestern forested test plot (SF1). The median ddf values for the open mires (OM1, OM2, and OM3) during 2015 were in the same range as found for the spruce forest (SF1 and SF2). The variation was exceptionally high in 2014 in test plots TZ1, TZ2, and SF2.

The highest ddf value (median 4.6 mm $d^{-1}$ $°C^{-1}$) was observed in the higher elevation plot at the transitional slopes in 2014, while the lowest ddf (median 2.0 mm $d^{-1}$ $°C^{-1}$) was observed for the low elevation mire in 2015.

For the test plots which were used in both years (OM2, SF1, SF2, and FL1) the highest melt rate (median 3.2 mm $d^{-1}$ $°C^{-1}$) was found at the forest line, followed by forest plots (median 2.6 mm $d^{-1}$ $°C^{-1}$) and the mire plot (median 2.3 mm $d^{-1}$ $°C^{-1}$). The median ddf for these plots was 3.66 mm $d^{-1}$ $°C^{-1}$ for 2014 and 2.44 mm $d^{-1}$ $°C^{-1}$ for 2015, with a coefficient of variation (CV) of 0.37 and 0.24, respectively

**Table 5. Calculated degree-day factor (ddf, mm $d^{-1}$ $°C^{-1}$) for each test point, plot and whole experimental area during 2014[1] and 2015[1]. OM = open mire, SF = spruce forest, FL = forest line, TZ = transitional zone (Adapted, with permission, from Paper I © 2018 Elsevier B.V.).**

| Site | 1 | 2 | 3 | 4 | 5 | Mean | Median |
|---|---|---|---|---|---|---|---|
| OM1 | - / 2.87 | - / 2.03 | - / NA | - / 2.59 | - / 2.59 | - / 2.52 | - / 2.59 |
| OM2 | 2.80 / 2.04 | 5.35 / 1.84 | 4.35 / 2.28 | NA / 1.83 | 3.23 / 2.28 | 3.93 / 2.05 | 3.79 / 2.04 |
| OM3 | - / NA | - / 2.75 | - / 2.29 | - / 3.45 | - / 2.34 | - / 2.71 | - / 2.55 |
| SF1 | 3.66 / 2.11 | 4.81 / 1.66 | 4.31 / NA | NA / 2.82 | 5.32 / 2.56 | 4.53 / 2.29 | 4.56 / 2.34 |
| SF2 | 2.56 / 2.39 | 2.59 / 2.42 | 2.18 / 2.88 | NA / 2.39 | 7.43[3] / 2.98 | 3.69 / 2.61 | 2.57 / 2.42 |
| FL1 | 3.54 / 3.16 | NA / 3.16 | 2.37 / 2.44 | 3.53 / 3.06 | NA / 4.25 | 3.14 / 3.21 | 3.54 / 3.16 |
| TZ1 | 2.84 / - | 5.82 / - | 8.91[2] / - | 2.38 / - | NA / - | 4.98 / - | 4.33 / - |
| TZ2 | 6.95 / - | 3.67 / - | 6.69 / - | 4.59 / - | 2.97 / - | 4.97 / -. | 4.59 / - |
| ALL | - | - | - | - | - | 4.28 / 2.57 | 3.66 / 2.44 |

[1] the first value is from 2014 and the second is from 2015

[2] Small brook observed at the logger location when fetching the loggers

[3] Hummock and snapped trees observed at the logger location when fetching the loggers

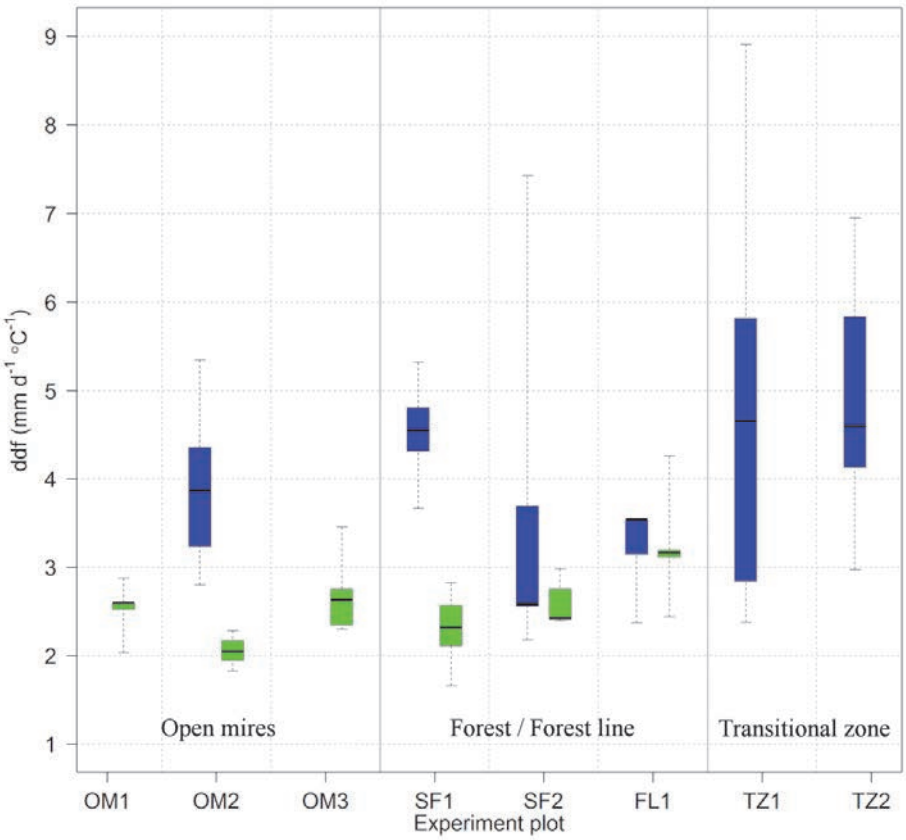


**Fig. 11. Boxplot of variation in calculated degree-factors (ddf) at test plots in 2014 (blue) and 2015 (green) (Reprinted, with permission, from Paper I © 2018 Elsevier B.V.).**

## 4.2 UAS provides high-resolution snow depth mapping that enables detailed analysis of snow cover variability and snow canopy interactions (Paper II)

### *4.2.1 Spatiotemporal variability of snow depth during accumulation and melt*

The difference between ultrasonic point measurement and snow depth maps generated using UAS-SfM showed high variability within and between experiment plots (Fig. 12 and Table 6). The median difference between the point sensor and all

test plots was positive at the beginning of snow accumulation (DEC-12) with a median of +5 cm and increasingly negative for the middle of snow accumulation (FEB-21), beginning of the melt (APR-03), and middle of the melt (APR-24) with medians of −3 cm, −9 cm and −22 cm, respectively.

This difference during the melt period was highest in the Mire plot with a median of −28 cm, but it was also high in the Mixed plot, with a median of −24 cm. The lowest differences were found in the Forest plot with a median of −8 cm compared to point measurement. Additionally, snow was observed to accumulate at the edges of open mires, next to forested areas, for all surveys. The central value and distribution of snow depth was similar between snow course reference measurements and UAS-SfM derived maps (Fig. 12), except for DEC-12, where the central value from snow course was lower.

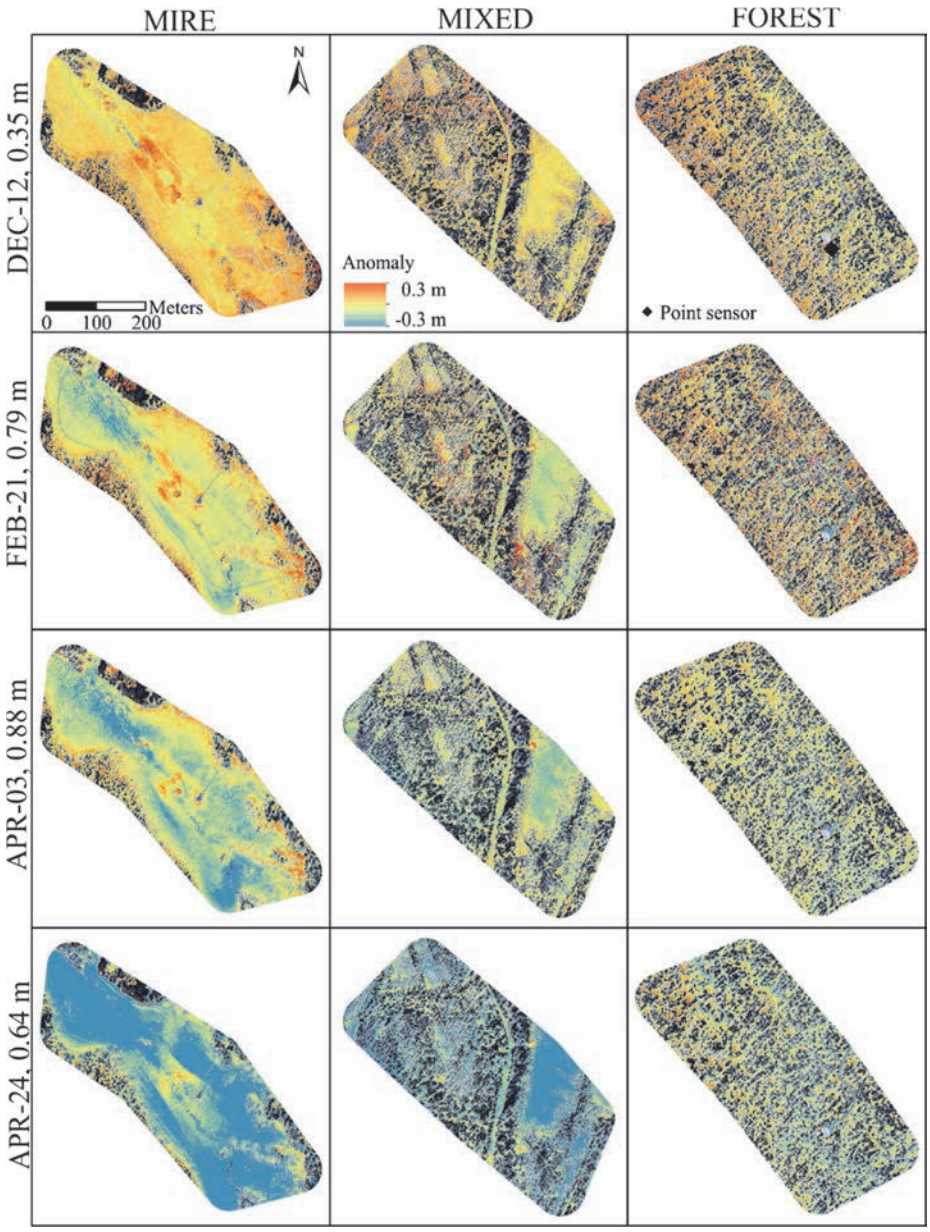


**Fig. 12. Snow depth difference between P4RTK based snow depth maps. The point measurement is marked with a black dot in the forest plot in the upper-right map. The point measurement snow depth on the day of the drone survey is shown in the y-label for each row (Reprinted, with permission, from Paper II © 2021 Authors).**

**Table 6. Median differences of snow depth (cm) between point measurement and UAS-SfM derived DoDs for each test site and snow course measurements (Adapted, with permission, from Paper II © 2021 Authors).**

| Date | Mire | Mixed | Forest | All | Snow line |
|---|---|---|---|---|---|
| Dec-12 | 6 | 4 | 5 | 5 | 1 |
| Feb-21 | -4 | -4 | 4 | -3 | -4 |
| Apr-03 | -11 | -9 | -4 | -9 | -3 |
| Apr-24 | -28 | -24 | -8 | -22 | -21 |

### *4.2.2 Land cover effect on snow depth variability*

Land cover specific differences of median snow depth between UAS-SfM derived snow depth maps and point measurement had a clear negative association with forest density (Fig. 13, Tables 7 and 8). The snow depth median for UAS-SfM derived snow depth maps was 5–6 cm higher than the point measurement for all Corine land cover types at the beginning of snow accumulation (DEC-12). For the following surveys (from FEB-21 to APR-03) this difference was mainly negative and the highest median differences, from −6 cm to −13 cm and from −2 cm to −5 cm, were found from open peatlands and transitional woodland/scrub. For mixed and coniferous forests, the median difference was from +1 cm to −5 cm and +1 cm to −6 cm, respectively. The differences between UAS-SfM derived snow depth maps and point measurement increased clearly in the middle of the melt period (APR-24), with the highest median difference of −32 cm in open peatlands and the lowest, −13 cm, in coniferous forests.

The variability within and between land cover types was positively associated with forest density and survey date (Fig. 13, Tables 7 and 8). The variability of snow depth (ranging between percentiles 5 and 95%, Table 8) was 35 cm and 33 cm for the mixed and coniferous forest at the beginning of snow accumulation (DEC-12) and increased throughout the snow season to 49 cm and 46 cm in the middle of the melt (APR-24). Similarly, for the open peatlands and transitional woodland/shrub, the range was 17 cm and 19 cm (DEC-12) and 42 cm (APR-24). A high variability range of 62–66 cm was observed for the coniferous and mixed forests in the middle of the snow accumulation season.

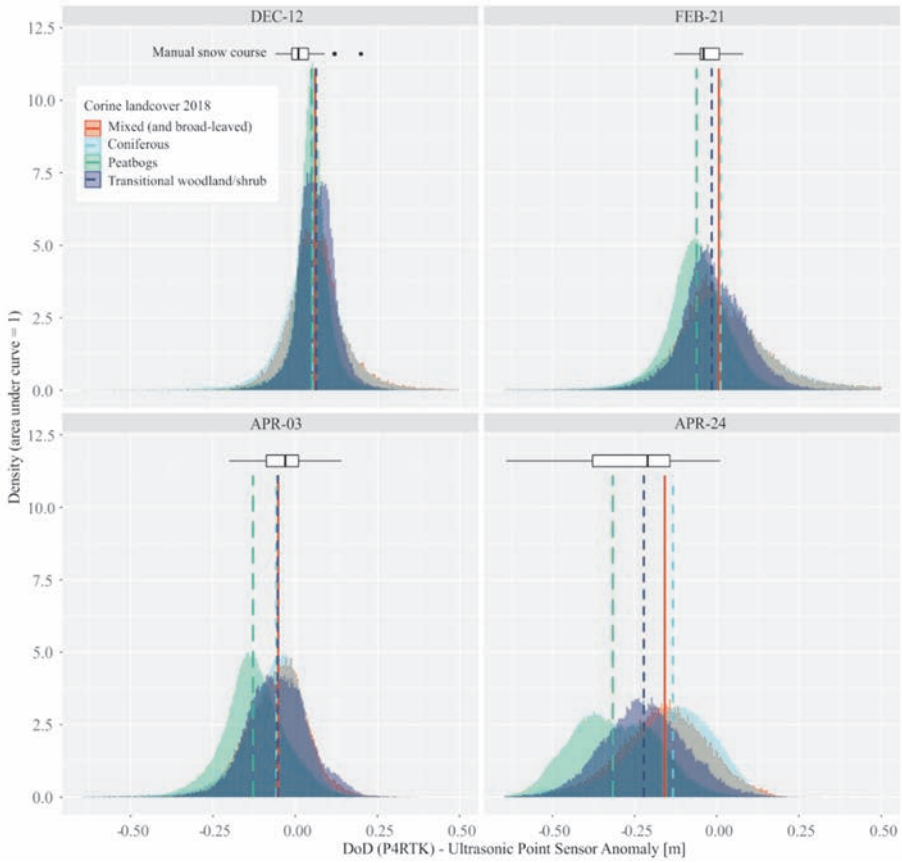


**Fig. 13. Snow depth histograms of the difference between P4RTK based snow depth maps and point measurement (Reprinted, with permission, from Paper II © 2021 Authors).**

**Table 7. Median and mean differences of snow depth in centimeters between point measurement and UAS-SfM derived DODs for each land cover type and snow course measurement (Adapted, with permission, from Paper II © 2021 Authors).**

| Date | Peatbogs | | Transitional woodland/scrub | | Mixed forest (and broadleaved) | | Coniferous forest | | Snow line | |
|---|---|---|---|---|---|---|---|---|---|---|
| | Median | Mean | Median | Mean | Median | Mean | Median | Mean | Median | Mean |
| Dec-12 | -5 | 5 | 6 | 7 | 6 | 14 | 5 | 7 | 1 | 2 |
| Feb-21 | -6 | -6 | -2 | -1 | 1 | 6 | 1 | 4 | -4 | -3 |
| Apr-03 | -13 | -13 | -5 | -5 | -5 | -8 | -6 | -9 | -3 | -3 |
| Apr-24 | -32 | -31 | -22 | -22 | -16 | -18 | -13 | -16 | -21 | -29 |

**Table 8. 5% and 95% percentiles of differences in snow depth in centimeters between point measurement and UAS-SfM derived DoDs and snow line measurements (Adapted, with permission, from Paper II © 2021 Authors).**

| Date | Peatbogs | | | Transitional woodland/scrub | | | Mixed forest (and broadleaved) | | | Coniferous forest | | | Snow line | | |
|---|---|---|---|---|---|---|---|---|---|---|---|---|---|---|---|
| | 5% | 95% | delta | 5% | 95% | delta | 5% | 95% | delta | 5% | 95% | delta | 5% | 95% | delta |
| Dec-12 | -4 | 13 | 17 | -3 | 16 | 19 | -8 | 27 | 35 | -11 | 22 | 33 | -4 | 11 | 15 |
| Feb-21 | -21 | 8 | 29 | -16 | 16 | 32 | -20 | 46 | 66 | -25 | 37 | 62 | -9 | 7 | 16 |
| Apr-03 | -28 | 4 | 32 | -21 | 11 | 32 | -24 | 9 | 33 | -28 | 7 | 35 | -17 | 9 | 26 |
| Apr-24 | -52 | -10 | 42 | -43 | -1 | 42 | -41 | 5 | 46 | -44 | 5 | 49 | -64 | -5 | 59 |

### *4.2.3 Vegetation interaction with snow depth*

The median of all snow depth values at a given distance from the canopy increased outwards from the canopy (Fig. 14). This increase was higher and reached further away from the canopy in more densely forested areas and during the melt period, compared to open areas and snow accumulation season. At the beginning and in the middle of snow accumulation (DEC-12 and FEB-21), the median snow depth increased by 3–5 cm to a distance of 1 m from the canopy within all landcover types. At the beginning of snowmelt (APR-03), the median snow depth increase was 6–7 cm in forested areas to a distance of 2.5 m from the canopy, while in open peatbogs and transitional woodland/scrub, the median snow depth increase remained at 3–5 cm with an increased distance of 1–2 m from the canopy. In the middle of the melt (APR-24), the median snow depth increased by 15 cm to a distance of 2.5 m from the canopy in conifer and mixed forest. In the open peatland and transitional woodland/scrub, the median snow depth increase was 5–6 cm to a distance of 1 m in peatland and 2 m in the transitional woodland/shrub. Generally,

the median snow depth was observed to decrease from the highest value with increased distance from the canopy.

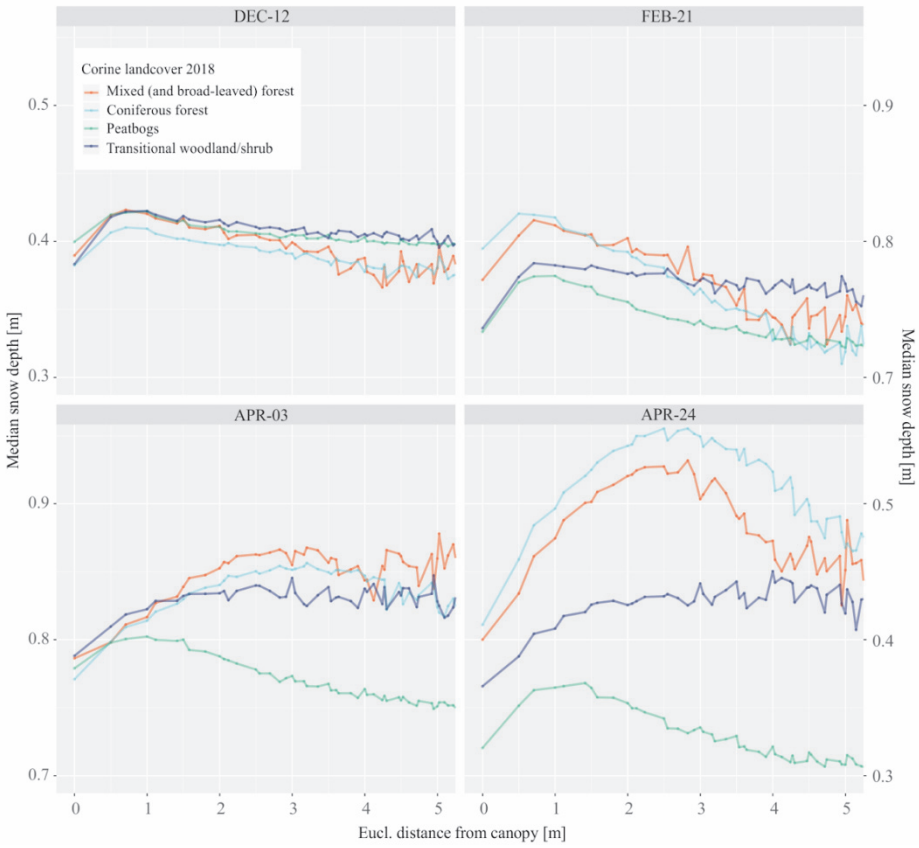


**Fig. 14. Snow depth against Euclidian distance from the canopy (tree mask) for different land cover types in test areas. The zero distance of the canopy in the figure is equal to the width of the buffer zone of 36 cm from the canopy (Reprinted, with permission, from Paper II © 2021 Authors).**

## 4.3 Snow conditions and snow to precipitation ratio dominates summer low flow regimes (Paper III)

### *4.3.1 Catchment storage and storage sensitivity of streamflow*

Catchment storage ($S_C$) and storage sensitivity of streamflow ($\varepsilon_S$) for low flow, calculated using recession analysis, showed considerable spatial variation between the study catchments (Fig. 15). In general, catchment storage increased when moving from the southwest coast towards the interior northeast of Finland, while the storage sensitivity of streamflow decreased. Plotted using a log-log scale, both storage indices were linearly related to the mean annual 7-day low flows during summer and winter periods (Fig. 16). Catchment storage had a positive relationship with 7-day low flows, while the relationship was negative for the storage sensitivity of streamflow, confirming that the hydrograph-derived indices reflect catchment flow characteristics. A stronger relationship was observed between summer low flow and the storage indices than for winter low flow.

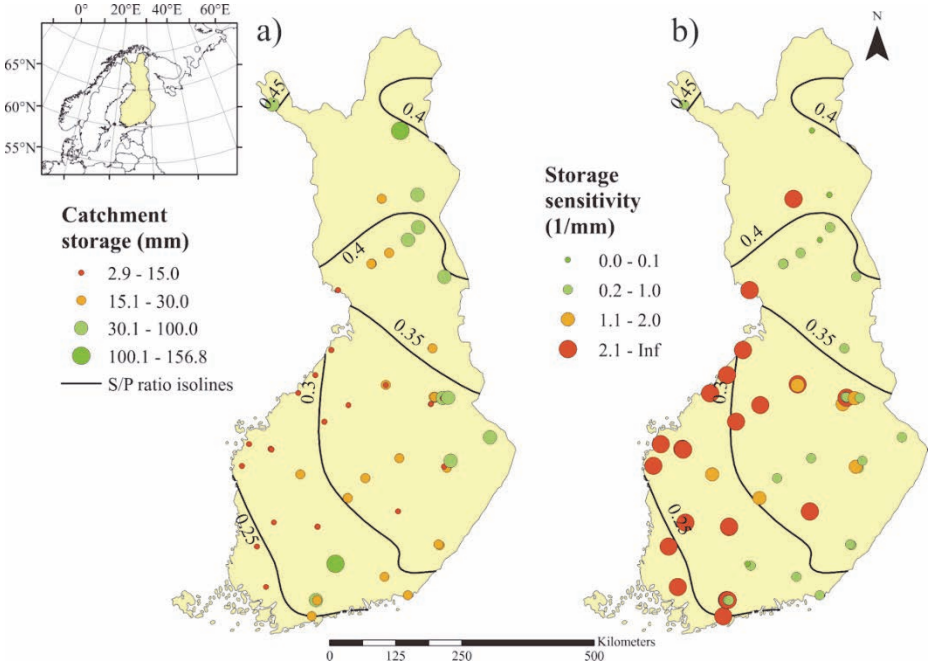


**Fig. 15. Calculated catchment water storage and storage sensitivity for low flow conditions in the study catchments (Reprinted, with permission, from Paper III © 2019 American Geophysical Union).**

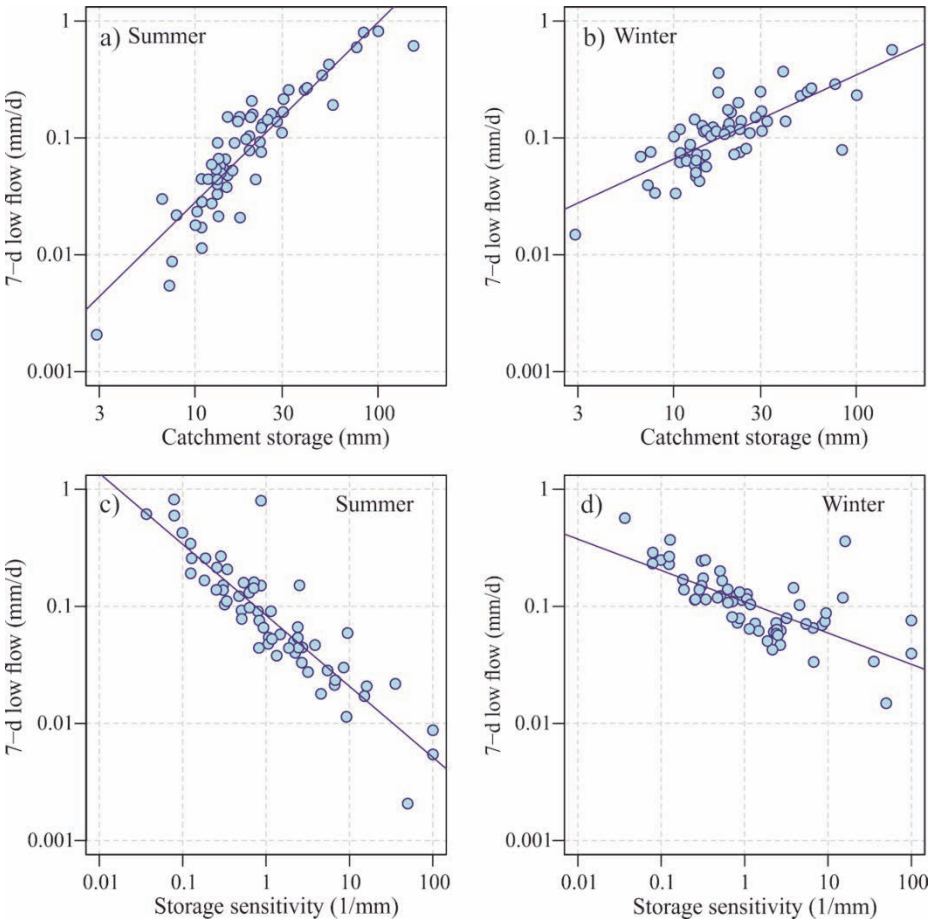


**Fig. 16. Catchment storage, storage sensitivity, and low from summer and winter (Reprinted, with permission, from Paper III © 2019 American Geophysical Union).**

### *4.3.2 Interactions between climate, snow, catchment characteristics, and low flows*

The first two principal components from the PCA, PC1 and PC2, that were selected for further analysis using the broken stick criterion, explained 42.1% and 16.6% of the variance in climate and catchment characteristics among the study catchments (Table 9). Based on the loadings (Table 9), PC1 was suggested to represent snow and climate conditions, with higher values associated with greater snow influence and colder air temperatures (Fig. 17). The loadings on PC1 were also high for mean

elevation, clay/silt soils, agriculture, and pristine peatlands, suggesting their covariance with climate. The proportion of pristine peatlands and mean elevation was positively associated with PC1, while for the proportion of agriculture and clay/silt soils the association was negative. PC2 showed the high loadings for drained and forested peatlands (Table 9), with higher values associated with their greater proportion (Fig. 17). The negative association with PC2 was found for mean slopes and forest on mineral soil, suggesting their covariation.

**Table 9. Summary of PCA of Climate and Catchment Characteristics[1] (Reprinted, with permission, from Paper III © 2019 American Geophysical Union).**

| Characteristics | PC1 | PC2 |
|---|---|---|
| Eigenvalue | 8.0 | 3.2 |
| % explained | 41.1 | 16.6 |
| Cumulative % explained | 41.1 | 58.7 |
| Mean elevation (MASL) | 0.29 | -0.16 |
| Mean slope (degrees) | -0.04 | -0.44 |
| Sand/gravel (%) | -0.11 | 0.00 |
| Clay/silt (%) | -0.26 | -0.09 |
| Till (%) | 0.21 | -0.01 |
| Drained peatland (%) | 0.09 | 0.43 |
| Pristine peatland (%) | 0.22 | 0.15 |
| Peatland total (%) | 0.21 | 0.41 |
| Agriculture (%) | -0.26 | 0.01 |
| Forest on mineral (%) | 0.06 | -0.28 |
| Forest on peat (%) | 0.16 | 0.44 |
| Lakes (%) | 0.09 | 0.04 |
| DoY[2] for Max SWE | 0.33 | -0.08 |
| DoY[2] for snow end | 0.32 | -0.12 |
| Climate elasticity (mm/mm) | -0.04 | 0.15 |
| Air temperature (°C) | -0.32 | 0.09 |
| Max SWE[3] (mm) | 0.33 | -0.02 |
| S/P ratio[4] (mm/mm) | 0.31 | -0.14 |
| P/PET[5] (mm/mm) | 0.25 | -0.23 |

[1] See Supporting Information Figure S5 for PCA biplot of climate and catchment characteristics and catchments in Paper III.

[2] Day of Year, [3] Snow Water Equivalent, [4] Snow to Precipitation ratio

[5] Precipitation/Potential Evaporation (Wetness index)

In GAM analyses, where PCs were used as predictor variables for storage and low flow indices, a clear negative association was observed between storage sensitivity

and PC1, representing the climate and snow (Fig. 17a). For catchment storage and summer 7-day low flows, the association was positive (Figs. 17b and 17c). The association was less clear for winter 7-day low flows (Fig. 17d). As suggested already by the PC1 loadings, color coding (Fig. 17) showed that catchments with a higher proportion of agriculture and clay/silt soils were in areas with warmer temperatures and less snow, indicated by the signs and strength in PC1 values. LOOCV analysis showed no significant changes in the shape of the response curves, which stayed inside the 2× standard error confidence bands (shown by shaded areas in Fig. 17) of the main GAMs (Figs. 17a–17d).

The high values of PC2 represented catchments with more drained/forested peatlands, whereas low values indicated a higher proportion of forest on mineral soil and higher slopes. The observed associations were negative between PC2 and catchment storage, and winter and summer low flows, with minor sensitivity in LOOCV (Figs. 17f–17h). No association was found between PC2 and storage sensitivity (Fig. 17e). Color-coded partial residuals showed outlier catchments with a higher proportion of clay/silt soil or agriculture had higher storage sensitivity and smaller storage volume (Figs. 17e and 17f). The partial residuals indicated a slight positive relationship between PC2 and storage sensitivity above a PC2 value of zero without those outliers (Fig. 17e).

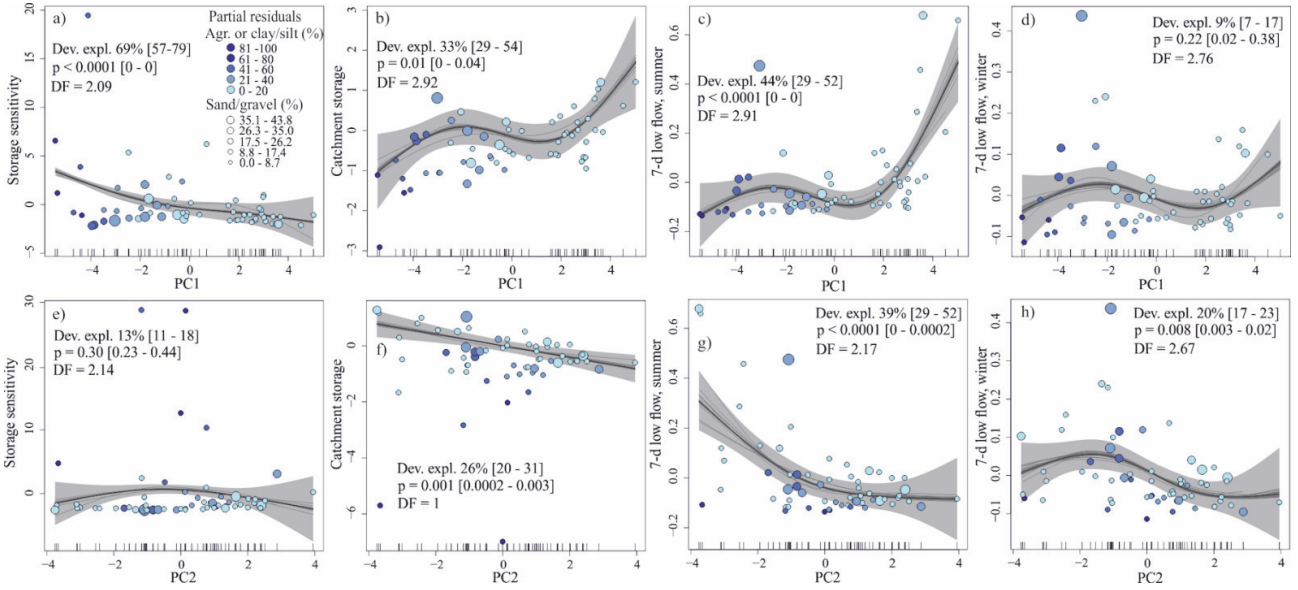


**Fig. 17. Generalized additive model-based response curves (black) for PC scores (a–d for PC1 and e–h for PC2) and (a, e) storage sensitivity ($\varepsilon_S$), (b, f) catchment storage ($S_C$), (c, g) 7-day summer low flow, and (d, h) 7-day winter low flow. Explained deviance (Dev. expl.; %), p-value, and degrees of freedom (DF) of the model are shown in each diagram, with ranges for explained deviance and p values from leave-one-out cross-validation in brackets. Response curves from leave-one-out cross-validation are shown in dark gray. Standardized partial residuals (unitless, shown on the y axis) are the estimates of the response variable using only the smooth term plus the residuals from the full model. Color coding for the partial residuals shows the percentage of agriculture and clay/silt soils, while size coding shows the percentage of sand/gravel soils. Tick marks on the x-axis indicate the location of the data points. PC = principal component (Reprinted, with permission, from Paper III © 2019 American Geophysical Union).**

The association observed between climate/snow (PC1) and 7-day low flow was investigated in more detail using the snow to precipitation (S/P) ratio. The S/P ratio was selected as the predictor variable for the GAMs because it was derived from the most consistent and longest data set on temperature and precipitation. The resulting GAM showed a strong and generally positive association between precipitation falling as snow (S/P ratio) and summer 7-day low flow (60% of deviance explained, $p < 0.001$) for the whole range of S/P ratio values (Fig. 18). A threshold where the association between S/P ratio and summer low flow began to strengthen was observed at an S/P ratio of 0.35. Above this threshold, the summer 7-day low flow started to increase rapidly. At S/P ratio values below 0.3, summer low flow started to decrease, while in between 0.3 and 0.35 the average impact was negligible. Outliers were observed at an S/P ratio of 0.29 where the catchment had the highest proportion of gravel/sand soil and at, 0.39 and 0.41, where the catchments contained heavily drained peatland used for peat extraction and forestry. Interestingly, no association between winter 7-day low flow and S/P ratio was observed. The results did not show high sensitivity in LOOCV (Fig. 18).

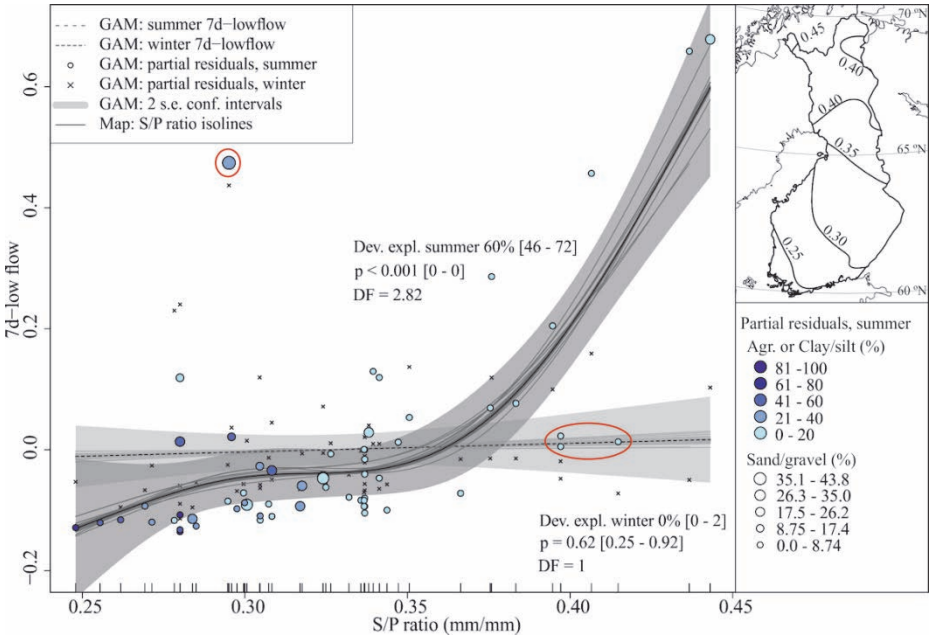


**Fig. 18. Generalized additive models (GAMs) of 7-day low flow (mm/day) in summer and winter explained using snow to total precipitation ratio (S/P, mm/mm). The relationship between 7-day summer low flow and S/P ratio is strong (p < 0.001, 60% of deviance explained), whereas the relationship with 7-day winter low flow is not significant (p > 0.6, 0.4% of deviance explained). Ranges for explained deviance and p values from leave-one-out cross-validation are in brackets after the values from the main model. Response curves from leave-one-out cross-validation are shown in dark gray. Standardized partial residuals (unitless) are shown on the y axis. Color coding for the partial residuals shows the percentage of agriculture and clay/silt soils, while size coding shows the percentage of sand/gravel soil. The shaded area shows the confidence interval of 2 standard errors, including the uncertainty of the overall mean. Tick marks on the x-axis indicate the location of the data points. Gaussian family with identity link function was used, and at most 3 degrees of freedom was allowed in GAM (n = 61). The insert shows a map of the study area with S/P isolines. Outliers are marked with red circles (Reprinted, with permission, from Paper III © 2019 American Geophysical Union).**

# 5 Discussion

## 5.1 Low-cost temperature sensors enable an analysis of snow conditions

The method developed in this thesis to analyze snow cover depletion and melt rates showed the potential to determine the spatiotemporal variation in different land cover conditions in Sub-Arctic regions (Paper I). Relatively strong agreement between temperature derived and reference station snowmelt timing was observed with minor differences, most likely caused by the small-scale variations in snow accumulation and melt speeds, depending on the microtopography and vegetation (Jost et al., 2007).

Snow accumulation and melt processes are mainly controlled by climate, topography, and vegetation (Jost et al., 2007; Liston, 2004; Pomeroy & Goodison, 1997). The analysis on variability in snowmelt rates and ablation dates showed that snow melted earlier in open areas (mires, transitional zones), while the snow melted last in forests at north-facing slopes. These observations are physically meaningful as snow ablation dates are associated with snow accumulation (Liston, 1999; Lundquist & Lott, 2010) and increased solar radiation in spring accelerating the melt (Gelfan et al., 2004). In contrast to observations in other studies showing increased snow accumulation in open areas due to canopy interception (Gelfan et al., 2004; Kozii et al., 2017), in this study, lower snow water equivalents were measured in open peatlands than forested areas. This indicates that northern peatlands accumulate less snow than forests, supporting other studies with similar observations (Koskinen et al., 1997; Kuusisto, 1984). An explanation could be that in cold conditions the snowflakes bounce from the accumulation surface, e.g., tree branches (Kozii et al., 2017), and are subject to wind redistribution in open areas for long time periods when the days are short (Gelfan et al., 2004). Moreover, particularly in groundwater-dominated open mires (fens), the early snowfall can melt into the ground because the ground can stay unfrozen later than mineral soils due to the high heat capacity of the water. The forested area at the north-facing slope is shaded from solar radiation slowing down the melt.

The observed variability of snowmelt in open areas compared to forested areas was low, this was also shown in UAS based snow maps in Paper II. However, these trends were inconsistent in 2015, likely influenced by the increased cloudiness and decreased global radiation in May 2015 compared to May 2014, which can equalize

the snowmelt rates (as also indicated by the differences in degree-day factors, see Fig. 11). The observed overall higher variability of snow cover depletion compared to within plot variation agrees with previous snow process studies, as the variability of the snow cover increases between land cover types and scale (Shook & Gray, 1996).

The calculated degree-day factors in this study combined all the melt processes into a single value for each temperature logger location. The calculated values corresponded to the range found in the literature (DeWalle & Rango, 2008; Hock, 2003; Kuusisto, 1984). The variability was considerably high, which was expected based on the variability observed on the measured snow properties, land cover, and topography at the logger locations. Higher degree-day factors and the plot variability between and within them observed in the winter of 2014 compared to 2015 can be explained by decreased cloudiness and increased global radiation amounts (not shown), which can increase the melt rates at areas exposed to solar radiation. The results were physically meaningful as the highest degree-day factors were found in south-facing, almost open slopes in the transitional zone, followed by open mires and forest line in 2014. Unexpectedly high values found in the forested plot at the south-eastern slope were equally as high as in the transitional zone. These high values could be related to relatively low canopy densities at these forested plots and observations in related literature indicating high degree-day variability for low canopy densities (Kuusisto, 1984). The results of this thesis highlight the challenges in using terrain-specific degree-day factors in distributed snow modeling and their dynamic behavior (Okkonen & Kløve, 2010) as there were substantive differences between study years and the values overlapped between different physiographical and vegetation types.

Reusser & Zehe (2011) used nine sensors with 15 cm spacing for snow depth and cold content estimation. Their approach provides more information on the temperature profile at a point and thus the moment when the cold content is zero can be estimated without additional calibration measurements. However, the SWE reference measurements are still needed, and the point measurements provided no information about micro-/local scale variation in the snow cover.

The advantages over other low-cost methods, such as manual probing, snow stakes, and automated cameras, is that the temperature data-based method is robust, requires low power, and offers continuous and temporally high-resolution temperature data from the snowpack. With more sensors used in a snow column and added wireless connection, even real-time information about the snow cover could be provided.

## 5.2 UAS provides high-resolution snow depth mapping that enables detailed analysis of snow cover variability and snow canopy interactions

The spatiotemporal coverage and resolution on snow process analysis were extended using UAS-SfM remote sensing techniques in Paper II. With GNSS-RTK equipped drones, the amount of fieldwork was substantially reduced as, in contrast to non-RTK, only one ground reference measurement is required to correct the possible offset of the surface maps. The cold air temperatures and short days in the subarctic winter conditions set requirements especially for the camera quality and timing of the surveys, highlighting the importance of planning the surveys.

High-resolution snow depth maps (Fig. 12) that compared well with conventional in-situ snow line measurements were successfully created for the whole snowy season, from December 2018 to April 2019. Snow depth maps covered larger areas compared to snow line measurements, providing extended and detailed distribution of the snow depth. Comparing UAS-SfM derived snow depth maps with point measurement data showed increasing differences during the snow season (from +5 cm to −32 cm) (Fig. 13), highlighting the potential for biased estimates of snow depth and presence during melt season if only point measurement data is used as a regional reference. This could have a substantial impact on simulated and predicted floods.

One essential novelty of this thesis was in the UAS-SfM based snow process analysis, especially in boreal landscapes which often comprise the mosaic of forested, transitional, and peatland vegetated areas. Removing the areas with canopy foliage using specific canopy masks provided a robust method to remove noisy sub- and near canopy areas, that are problematic to the UAS-SfM method, and are not reported in the available literature to date. Instead, other studies have focused on the accuracy of the method in mostly mountainous, temperate forests and tundra land covers, while the snow process considerations (Fernandes et al., 2018; Harder et al., 2020; Lendzioch et al., 2016) have been limited. Moreover, the existing studies have typically been applied to single campaigns or melt season while this study covered the period from early snow accumulation to the middle of the melt season. This allowed quantification and comparison of differences in snow depth patterns and snow-canopy interaction in high resolution and different snow conditions for multiple land cover types.

Increasing snow depth variability within and between land cover types was observed when the snow season progressed (Fig. 13, Tables 7 and 8). Higher snow

depths and variability were generally observed in forests compared to open peatlands, like in Paper I, and matching the findings in (Jost et al., 2007) for forests and clear-cuts.

Interestingly, observations from snow depth maps for early snow accumulation in December show similar snow depths between all land cover types. This may be a result of snow trapping in low vegetation hindering wind redistribution in open areas and there being less time for post-depositional processes to influence snow depth (Liston & Sturm, 2002; Pomeroy et al., 2002). Another interesting observation was that the median snow depth for all land cover types was +5–6 cm higher than in reference snow course and point measurements in December. Fernandes et al. (2018) observed a similar phenomenon and attributed it to misclassified snow surface caused by snow-covered low vegetation, also visible in the orthophotos created in this study (not shown). With the progress of snow season, wind transport and deposition processes (Hiemstra et al., 2002; Ketcheson et al., 2012) were revealed, as observed snow depths during sequential campaigns (from February to April) showed lower values in open peatlands and higher values at their edges (Fig. 12, Tables 7 and 8). An exception from the general snow depth variability patterns was observed in mixed and conifer forests in the middle of the snow accumulation on 21$^{st}$ February (Fig. 13, Table 8). During this survey, the trees were snow-covered, which can be challenging for the UAS-SfM method and can result in anomalously high snow depths near tree canopies, especially for broad-leaved trees because only leafless branches could be identified using supervised classification, leaving gaps in tree masks.

In the middle of the melt period on 24$^{th}$ April, the observed variability was highest within and between land cover types, highlighting findings in the literature that show snow depth variability increasing with time and scale (López-Moreno et al., 2015; Neumann et al., 2006). A clear pattern of increase in snow depth with increased vegetation density was observed (Fig. 13, Table 7), while the snow depth variability within land cover types was similar. These observations can be explained by lower initial snow depths in open peatlands and transitional woodland/scrub and their exposure to solar radiation compared to mixed and coniferous forests (Hardy et al., 1997; Lundquist & Lott, 2008).

In the middle of the melt period specifically, but also at the end of the snow accumulation period, the snow depths were substantially lower than the ultrasonic point measurement for all land covers, highlighting the poor representativeness of point measurements even for similar land cover types (Figs 12 and 13). Compared to manual snow line measurements, the central value and variability of the UAS-

SfM derived snow depth maps were generally similar, but the spatial coverage was substantially expanded. Nonetheless, this analysis suggests that snow line, a widely used operational method for characterizing bulk snowpack (Pirazzini et al., 2018) produces a realistic picture of areal snow depth and its variability.

In a more detailed investigation of interaction between snow cover and vegetation, a systematic snow depth increase of 2–15 cm from the canopy edge was observed throughout the snow season (Fig. 14). In literature, similar observation has been made for white spruce in a stand of trembling aspen (Pomeroy & Goodison, 1997), in the sub-alpine forest (Musselman et al., 2008) and near larch trees in Kananaskis, AB, Canada (Harder et al., 2020).

Interestingly the observed median snow depth had a peak value around 1m from the tree mask during accumulation season, but this peak distance increased by up to 2.5 m in the middle of the melt period, and after the peak, the snow depth was decreased (Fig. 14). Moreover, the increase in snow depth from canopy edge to its peak value was amplified from +2 cm on 21$^{st}$ December to +15 cm on 24$^{th}$ April, especially for conifer and mixed forests, less so for mire, and not at all for transitional woodland/shrub. At the present time, this temporally changing canopy-snow interaction is not documented elsewhere.

Generally, canopy interception and sublimation can hinder the accumulation of snow under the canopy and fringe area, but forest openings with dimensions from 2–5 times the height of the surrounding forest tend to collect snow (Pomeroy et al., 2002). For open peatlands, this peaking could be explained by wind transport processes and deposition near canopies (Kuusisto, 1984; Vajda et al., 2006) also observed in snow depth maps (Fig. 12). For transitional woodland/scrub, the behavior was inconsistent and could be explained by the limited canopy effect compared to forested areas. In mixed and conifer forest land cover, the snow depth increase and distance of the peak snow depth increased at the end of snow accumulation, 3$^{rd}$ April, and especially for the middle of the melt period, 24$^{th}$ April (Fig. 14). This intensified peaking could be explained by the increased longwave melt energy from the canopy affecting areas progressively further away from it (Faria et al., 2000; Lundquist et al., 2013). The decreased snow depths after 3 m from the canopy could relate to direct solar radiation affecting the northern side of the forest openings, while the southern sides are protected by shadows from the trees (Essery et al., 2008). This may cause the increase in the variance in snow depth and the general increase melt in openings but needs further investigations. Fig. 19 summarizes the observed snow processes for different land cover types and snow-canopy interaction for snow accumulation and melt period.

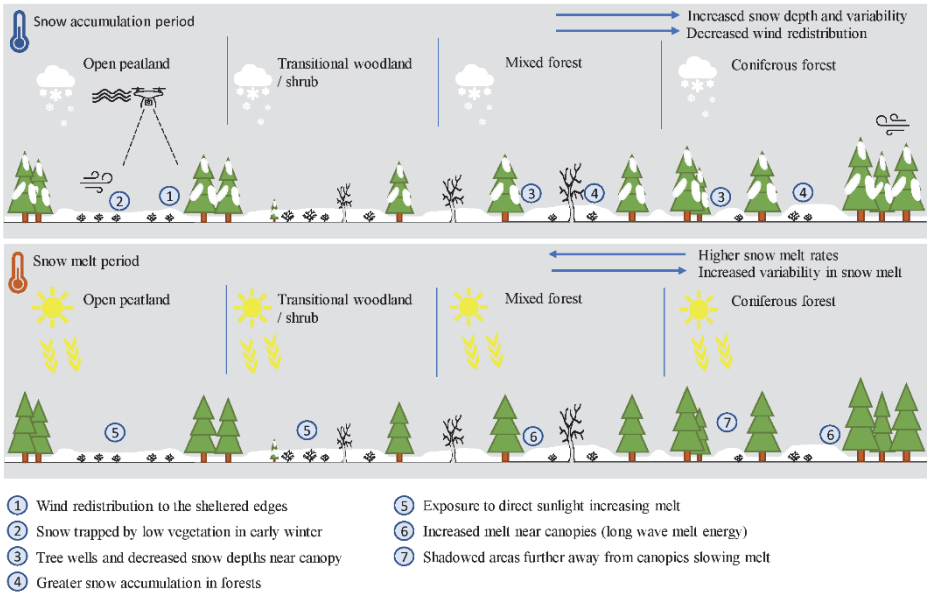


**Fig. 19. Observed snow accumulation and melt processes for different land cover types using the UAS-SfM method (Reprinted, with permission, from Paper II © 2021 Authors).**

## 5.3 Snow conditions and snow to precipitation ratio dominates summer low flow regimes

Notable spatiotemporal variation was observed in catchment storage and sensitivity and their association with low flows in the examined 61 catchments in the Finnish small basin research network. Previous studies suggest that long-term interactions between climate, geology, and vegetation determine the catchment's natural hydrological response, later modified by land-use changes or other anthropogenic influences (Blöschl et al., 2013). Indeed, in this thesis, coastal low elevation areas with younger soils and a lower snow to precipitation ratio showed lower catchment storages and higher sensitivity of streamflow (Fig. 15), indicating these areas are already vulnerable to climate variability and land-use changes. In contrast, higher catchment storages and lower storage sensitivity of streamflow were generally found for forested northern and eastern areas with glacial till and peat soils under current conditions, indicating greater resistance to changes.

Plotting the calculated storage indices and seven-day in log-log scale (Fig. 16), low flow showed a strong non-linear association between the variables, exposing the connection between catchment storage and ecologically and socioeconomically important low flows found in previous studies (Eltahir & Yeh, 1999). This supports the idea that storage sensitivity of streamflow could be used as a measure for catchment vulnerability (Berghuijs et al., 2016). The stronger association found between storage indices and seven-day summer low flows compared to winter low flows could be explained by different dominating hydrological processes in winter and summer, and seasonal precipitation patterns (see Paper III for more details).

In the statistical analysis, climate factors and snow, represented by PC1 (Table 9), showed a strong association with catchment storage properties and low flow, especially in summer low flow (Fig. 17), backed by previous studies suggesting that climate is the first-order control on hydrology (Devito et al., 2005). Negative loadings with air temperature in PC1 suggested that in warmer regions with less snow (high loads for PC1) and higher evapotranspiration (moderate load in PC1 through wetness index) the catchment storage was decreased, and sensitivity of streamflow was increased. The association found between climate and streamflow is essential information for managing and mitigating the present and future pressures from climate and land-use changes. Especially by supporting low flows that are directly supporting stream ecosystems (Poff et al., 1997).

A strong association between S/P (snow to precipitation) ratio and summer low flows was observed (Fig. 18), shown elsewhere in recent literature (Godsey et al., 2014; Jenicek et al., 2016). S/P ratio was observed to correlate strongly with other climate and land cover variables (see Paper III), which impeded the identification of hydrological controls. However, the suggested controlling role of temperature-dependent S/P ratio on storage properties and low flow can be considered meaningful, based on the literature and process knowledge. The high SWE and late snowpack depletion in the northern boreal region potentially fill the soil storage and recharge the groundwater storage closer to the summer growing season, also supporting low flows during summer months when the evapotranspiration demand is high.

A clear threshold for S/P in supporting summer low flows was found (Fig. 18). A flattening relationship between S/P ratio and 7-day summer low flow is showed for S/P ratio values lower than 0.35. This observation strongly suggests that climate, and snow especially, dominate the hydrological regime above this S/P threshold, as the higher snowmelt induced storage recharge and lower evapotranspiration due to the shorter growing season in higher latitudes enabling the catchment to sustain

higher summer low flows. Below the 0.35 S/P threshold, temperature, rainfall, and the physiographical properties of catchments exert more direct control on the flow regime. These findings suggest that catchments at the S/P threshold zone can be considered especially sensitive to near-future changes in snow cover because the buffer for climate variability will be reduced by decreased snow storage. The geographical location of this S/P threshold zone is expected to move northeast in Fennoscandia in a warming climate (Mudryk et al., 2020). Similarly, areas most sensitive to changes in hydrology resulting from climate change can be found in many boreal and Arctic regions, especially in coastal areas (Prowse et al., 2015). Furthermore, changes in the S/P ratio threshold can lead to a discrepancy between supply and demand for water resources in a larger proportion of the boreal zone, which can have substantial impacts on ecology (Mustonen et al., 2018; Vörösmarty et al., 2010) and water security (Berghuijs et al., 2014). A less remarkable threshold was observed at an S/P ratio of 0.3. Below this threshold, summer low flows are already sensitive to climate variability, but at the same time the catchment characteristics seem to gain importance as clay/silt soils and agricultural areas are more abundant (Fig. 17, color coding) in the catchments concerned.

The loadings for PC1 showed covariation with certain catchment characteristics, suggesting an increase in their role in hydrology relative to climate. The catchments with the smallest storage and highest storage sensitivity were located at lower elevations (Table 9, Fig. 17). In these areas, post-glacial silt/clay sea sediments extending up to 100–200 km inland affect the soil, land use, and vegetation properties. Consequently, agricultural areas are often located on these fertile, alluvial, low-permeability clay/silt soils (both loaded in PC1), decreasing the water storage by land drainage and increasing water demand. These findings suggest that, while climate remains the primary control on hydrology in these lowland areas, catchment characteristics have a relatively higher influence than in the snow-dominated regions. In contrast, the catchments with the highest storage and the lowest storage sensitivity were found at higher elevations in the north and interior of Finland, where surface geology is dominated by basal till and peatlands are more abundant (Fig. 17). The loadings from till soils and pristine peatlands in PC1 were positive and moderate (Table 9), suggesting their interaction with the climate in supporting storage and summer low flows.

Similar findings for till soils were found for boreal Canada, where the moderate depth of basal till was observed to maintain low flow (Buttle & Eimers, 2009; Devito et al., 1996). The finding for pristine peatlands increasing storage and low flows are meaningful as they can buffer the influence of changes in climate on

streamflow, as there are several feedbacks in peatland systems for moderating water stresses (Waddington et al., 2015). This can be associated with increased groundwater outflow from the catchment. Moreover, peatlands are often located in groundwater discharge areas (Winter & Woo, 1990), which are often associated with increased baseflow in the catchment. However, further investigation with a larger dataset is required. In contrast to pristine peatlands, the loadings for drained and forested peatlands in PC2 (Table 9) suggest a decrease in catchment storage and both summer and winter low flows (Fig. 17), while the existing evidence has been inconclusive (Bacon et al., 2017; Holden et al., 2004). This indicates that peatland restoration could improve hydroecological conditions at the catchment scale, which is important information for policymakers. PC2 was also loaded strongly by mean slope, which suggests that catchment storage and low flows are greater in catchments with more variable topography and that drained peatlands are usually found on relatively flat terrain. Like recent findings by (Karlsen et al., 2016), increased storage properties and low flows at the catchment scale are indicated for forests on mineral soil by its moderate loadings in PC2.

# 6 Conclusions and future recommendations

This thesis combined development and testing new in-situ and remote sensing snow measurement methods with snow process analysis in the sub-arctic area. Both temporal and spatial variability in snow cover was addressed in high resolution. Additionally, a long-term dataset from the small basin network in Finland was used to investigate the impact of climate, snow, and climate characteristics on runoff, specifically low flow, and catchment sensitivity to changes. The high temporal-resolution data from in-situ, low-cost temperature loggers, with the algorithm developed, was found to provide relatively reliable and accurate data on spatiotemporal and inter-annual variations in snow cover ablation and melt rates in different boreal landcover types. Novel field evidence highlighted the dynamic nature of the snowmelt rates depending on the weather conditions, as the magnitude and variability of melt rates were substantially higher in spring with lower cloudiness. It was also possible to determine the melt rates at the end of the snowmelt period, which can be the most important period concerning the snowmelt-derived runoff. Depending on the local snow conditions, such as the thickness of the snowpack, multiple temperature sensors in a snow column could be used to additionally measure snow accumulation and melt rates for the whole snow season. The method could be used as a tool for measuring snowpack variations in previously ungauged or remote basins. Combined with continuous snow density measurements, the accuracy of the melt rate detection could be further improved by adding wireless connectivity, meaning real-time information on the snow conditions could be acquired.

The relatively low-cost UAS-SfM method successfully captured the snow depth variability in a mosaic of boreal landscape throughout the snow season with a very high spatial resolution with a larger coverage area. Forested land cover is known to be challenging for UAS-SfM snow remote sensing as the canopies are a hinderance to the sight under trees, and in winter conditions, the snowy canopies can cause abnormal snow depths in and near the tree canopies. The tree masks generated using survey data from spring, when the snow was melted from the canopies, were found to be an excellent way to remove the problematic canopy areas and areas immediately next to the canopies. The results highlight the potential of the UAS-SfM to be used for the detailed study of snow depth in multiple land cover types and snow-vegetation interactions in boreal sub-arctic conditions. The method can be used to extend the spatial scale of snow course measurements, especially for snow depth, in snow model calibration and validation in catchment-

scale models, and improved forecasting for operational and decision-making purposes.

The snow process analysis using temperature logger-derived data indicated that snow ablation occurred earlier in open peatlands and areas with low canopy density compared to more densely forested areas, with consistent results from the UAS-SfM based data. Snowmelt rates were found to be higher in open and sparsely forested areas at higher elevations, while peatlands and forested areas had lower values. The differences in melt rates were highlighted in the study spring with higher measured solar radiation and lower cloudiness. The UAS-SfM derived snow depth maps enabled a more spatially detailed study of the snow processes with high resolution. It is a method which can be recommended to be used in future studies. The differences in snow depth variability increased between and within the land cover types with the progress of the snow season, being highest during snowmelt. We identified multiple theoretically known snow processes and interactions between snow and vegetation, such as canopy interception and wind transport with deposition of snow at forest edges, for forested and peatland areas. The effect of decreased snow accumulation below canopies extending outside the immediate canopy was also shown in high resolution and a spatially extensive analysis.

With a warming climate, snow conditions are changing rapidly, with severe impacts on hydrological conditions in boreal regions. In this thesis, some geographical variation in the resilience and sensitivity of boreal catchments in Finland was detected. The findings suggest that, in a warming climate, the changes in hydrological processes related to snow conditions will be pronounced at a certain S/P ratio threshold, highlighting the strong connectivity between snow and ecologically important summer low flows. Pristine peatlands were indicated to support low flows but further analysis with a larger dataset is required. Peatland drainage was found to decrease catchment storage and low flows during both summer and winter, indicating that peatland restoration could improve hydroecological conditions at the catchment scale, which is important information for policymakers. The results can be used to mitigate the impacts of climate change and to guide land-use management in similar boreal and high-latitude regions where rapid climate change is projected.

Based on the results presented in this thesis, the following research and development topics would further advance the snow measurement techniques and understanding of snow hydrology:

- The data from temperature loggers should be studied further with streamflow data and aerial temperature and machine learning. Such work could reveal connections that could be used in water resource management, and flood predictions especially. Moreover, wireless sensors could be applied to gain real-time data on snow conditions in societally critical areas.
- More efforts should be put into a new lightweight and low-cost camera/sensor development for Unmanned Aerial Systems. Laser-based techniques would improve/enable measurements, especially in forested environments where visible light propagation is blocked by the vegetation. While snow depth can be used as a proxy for determining the snow water equivalent needed in the analysis of the hydrological condition, future development is suggested to develop and test sensors that can be used to directly measure snow water equivalent using the drone. Sensors working with radio-frequencies could help determine the snow water equivalent on a high spatial scale, which could be used in spatially distributed hydrological model calibration and validation.
- The observational snow cover data from new snow measurement methods should be further studied to investigate their value for hydrological modelling, which is needed to address water availability in a changing climate.
- Future studies on the connectivity between streamflow, climate, and catchment characteristics should be extended to larger northern hemisphere regions, to find possible larger patterns in how snow conditions impact catchment storage and streamflow.

# List of references


Aitchison, C. W. (2001). The effect of snow cover on small animals. In H. G. Jones, J. W. Pomeroy, D. A. Walker, & R. W. Hoham (Eds.), *Snow ecology: An interdisciplinary examination of snow-covered ecosystems.* (pp. 229–265). Cambridge University Press.

Arciniega-Esparza, S., Breña-Naranjo, J. A., & Troch, P. A. (2017). On the connection between terrestrial and riparian vegetation: the role of storage partitioning in water-limited catchments. *Hydrological Processes*, *31*(2), 489–494. https://doi.org/10.1002/hyp.11071

Bacon, K. L., Baird, A. J., Blundell, A., Bourgault, M. A., Chapman, P. J., Dargie, G., Dooling, G. P., Gee, C., Holden, J., Kelly, T., McKendrick-Smith, K. A., Morris, P. J., Noble, A., Palmer, S. M., Quillet, A., Swindles, G. T., Watson, E. J., & Young, D. M. (2017). Questioning ten common assumptions about peatlands. *Mires and Peat*, *19*, 1–23. https://doi.org/10.19189/MaP.2016.OMB.253

Barnett, T. P., Adam, J. C., & Lettenmaier, D. P. (2005). Potential impacts of a warming climate on water availability in snow-dominated regions. *Nature*, *438*(7066), 303–309. https://doi.org/10.1038/nature04141

Berghuijs, W. R., Hartmann, A., & Woods, R. A. (2016). Streamflow sensitivity to water storage changes across Europe. *Geophysical Research Letters*, *43*(5), 1980–1987. https://doi.org/10.1002/2016GL067927

Berghuijs, W. R., Woods, R. A., & Hrachowitz, M. (2014). A precipitation shift from snow towards rain leads to a decrease in streamflow. *Nature Climate Change*, *4*(7), 583–586. https://doi.org/10.1038/nclimate2246

Blöschl, G., Sivapalan, M., Wagener, T., Viglione, A., & Savenije, H. (Eds.). (2013). *Runoff Prediction in Ungauged Basins*. Cambridge University Press. https://doi.org/10.1017/CBO9781139235761

Blume-Werry, G., Kreyling, J., Laudon, H., & Milbau, A. (2016). Short-term climate change manipulation effects do not scale up to long-term legacies: effects of an absent snow cover on boreal forest plants. *Journal of Ecology*, *104*(6), 1638–1648. https://doi.org/10.1111/1365-2745.12636

Bonan, G. B., Pollard, D., & Thompson, S. L. (1992). Effects of boreal forest vegetation on global climate. *Nature*, *359*(6397), 716–718.

Brown, R. D., & Robinson, D. A. (2011). Northern Hemisphere spring snow cover variability and change over 1922-2010 including an assessment of uncertainty. *Cryosphere*, *5*(1), 219–229. https://doi.org/10.5194/tc-5-219-2011

Brutsaert, W. (2008). Long-term groundwater storage trends estimated from streamflow records: Climatic perspective. *Water Resources Research*, *44*(2), 1–7. https://doi.org/10.1029/2007WR006518

Brutsaert, W., & Nieber, J. L. (1977). Regionalized drought flow hydrographs from a mature glaciated plateau. *Water Resources Research*, *13*(3), 637–643. https://doi.org/10.1029/WR013i003p00637

Buhler, Y., Adams, M. S., Bosch, R., & Stoffel, A. (2016). Mapping snow depth in alpine terrain with unmanned aerial systems (UASs): Potential and limitations. *Cryosphere*, *10*(3), 1075–1088. https://doi.org/10.5194/tc-10-1075-2016

Buttle, J. M., & Eimers, M. C. (2009). Scaling and physiographic controls on streamflow behaviour on the Precambrian Shield, south-central Ontario. *Journal of Hydrology*, *374*(3–4), 360–372. https://doi.org/10.1016/j.jhydrol.2009.06.036

Castle, S. L., Thomas, B. F., Reager, J. T., Rodell, M., Swenson, S. C., & Famiglietti, J. S. (2014). Groundwater depletion during drought threatens future water security of the Colorado River Basin. *Geophysical Research Letters*, *41*(16), 5904–5911. https://doi.org/10.1002/2014GL061055

Clark, M. P., Hendrikx, J., Slater, A. G., Kavetski, D., Anderson, B., Cullen, N. J., Kerr, T., Örn Hreinsson, E., & Woods, R. A. (2011). Representing spatial variability of snow water equivalent in hydrologic and land-surface models: A review. *Water Resources Research*, *47*(7). https://doi.org/10.1029/2011WR010745

Cohen, J., Lemmetyinen, J., Pulliainen, J., Heinila, K., Montomoli, F., Seppanen, J., & Hallikainen, M. T. (2015). The Effect of Boreal Forest Canopy in Satellite Snow Mapping-A Multisensor Analysis. *IEEE Transactions on Geoscience and Remote Sensing*, *53*(12), 6593–6607. https://doi.org/10.1109/TGRS.2015.2444422

De Michele, C., Avanzi, F., Passoni, D., Barzaghi, R., Pinto, L., Dosso, P., Ghezzi, A., Gianatti, R., & Vedova, G. Della. (2016). Using a fixed-wing UAS to map snow depth distribution: An evaluation at peak accumulation. *Cryosphere*, *10*(2), 511–522. https://doi.org/10.5194/tc-10-511-2016

Deems, J. S., & Painter, T. H. (2006). Lidar measurement of snow depth: accuracy and error sources. *Proceedings of the International Snow Science Workshop*, *330*, 1–6.

Deems, J. S., Painter, T. H., & Finnegan, D. C. (2013). Lidar measurement of snow depth: A review. *Journal of Glaciology*, *59*(215), 467–479. https://doi.org/10.3189/2013JoG12J154

Devito, K. J., Creed, I., Gan, T., Mendoza, C., Petrone, R., Silins, U., & Smerdon, B. (2005). A framework for broad-scale classification of hydrologic response units on the Boreal Plain: Is topography the last thing to consider? *Hydrological Processes*, *19*(8), 1705–1714. https://doi.org/10.1002/hyp.5881

Devito, K. J., Hill, A. R., & Roulet, N. (1996). Groundwater-surface water interactions in headwater forested wetlands of the Canadian Shield. *Journal of Hydrology*, *181*(1–4), 127–147. https://doi.org/10.1016/0022-1694(95)02912-5

Devito, K. J., Hokanson, K. J., Moore, P. A., Kettridge, N., Anderson, A. E., Chasmer, L., Hopkinson, C., Lukenbach, M. C., Mendoza, C. A., Morissette, J., Peters, D. L., Petrone, R. M., Silins, U., Smerdon, B., & Waddington, J. M. (2017). Landscape controls on long-term runoff in subhumid heterogeneous Boreal Plains catchments. *Hydrological Processes*, *31*(15), 2737–2751. https://doi.org/10.1002/hyp.11213

DeWalle, D. R., & Rango, A. (2008). *Principles of snow hydrology*. Cambridge University Press.

Dietz, A. J., Kuenzer, C., Gessner, U., & Dech, S. (2012). Remote sensing of snow - a review of available methods. *International Journal of Remote Sensing*, *33*(13), 4094–4134. https://doi.org/10.1080/01431161.2011.640964

Dixon, R. K., Brown, S., Houghton, R. A., Solomon, A. M., Trexler, M. C., & Wisniewski, J. (1994). Carbon pools and flux of global forest ecosystems. *Science*, *263*(5144), 185–190. https://doi.org/10.1126/science.263.5144.185

Earman, S., Campbell, A. R., Phillips, F. M., & Newman, B. D. (2006). Isotopic exchange between snow and atmospheric water vapor: Estimation of the snowmelt component of groundwater recharge in the southwestern United States. *Journal of Geophysical Research*, *111*(D9), D09302. https://doi.org/10.1029/2005JD006470

Eltahir, E. A. B., & Yeh, P. J. F. (1999). On the asymmetric response of aquifer water level to floods and droughts in Illinois. *Water Resources Research*, *35*(4), 1199–1217. https://doi.org/10.1029/1998WR900071

Essery, R., Bunting, P., Hardy, J., Link, T., Marks, D., Melloh, R., Pomeroy, J., Rowlands, A., & Rutter, N. (2008). Radiative transfer modeling of a coniferous canopy characterized by airborne remote sensing. *Journal of Hydrometeorology*, *9*(2), 228–241. https://doi.org/10.1175/2007JHM870.1

Faria, D. A., Pomeroy, J. W., & Essery, R. L. H. (2000). Effect of covariance between ablation and snow water equivalent on depletion of snow-covered area in a forest. *Hydrological Processes*, *14*(15), 2683–2695. https://doi.org/10.1002/1099-1085(20001030)14:15<2683::AID-HYP86>3.0.CO;2-N

Feiccabrino, J., & Lundberg, A. (2008). Precipitation phase discrimination in Sweden. In R. Hellström & S. Frankenstein (Eds.), *65th Eastern snow conference* (pp. 239–254). https://www.easternsnow.org/esc-2008

Fernandes, R., Prevost, C., Canisius, F., Leblanc, S. G., Maloley, M., Oakes, S., Holman, K., & Knudby, A. (2018). Monitoring snow depth change across a range of landscapes with ephemeral snowpacks using structure from motion applied to lightweight unmanned aerial vehicle videos. *Cryosphere*, *12*(11), 3535–3550. https://doi.org/10.5194/tc-12-3535-2018

Finger, D. (2018). The value of satellite retrieved snow cover images to assess water resources and the theoretical hydropower potential in ungauged mountain catchments. *Jokull*, *68*(December 2018), 47–66.

Finger, D., Vis, M., Huss, M., & Seibert, J. (2015). The value of multiple data set calibration versus model complexity for improving the performance of hydrological models in mountain catchments. *Water Resources Research*, *51*(4), 1939–1958. https://doi.org/10.1002/2014WR015712

Finn, D. S., Bonada, N., Múrria, C., & Hughes, J. M. (2011). Small but mighty: Headwaters are vital to stream network biodiversity at two levels of organization. *Journal of the North American Benthological Society*, *30*(4), 963–980. https://doi.org/10.1899/11-012.1

Finnish Environment Institute. (2020). *CORINE Land Cover 2018 [Data file]*. https://paikkatieto.ymparisto.fi/lapio/latauspalvelu.html

Finnish Meteorological Institute. (2020). *Climate-Snow statistics*. http://en.ilmatieteenlaitos.fi/snow-statistics

Finnish Meteorological Institute. (2021). *FMI_CLIMGRID [Data file]*. https://paituli.csc.fi/download.html

Fujihara, Y., Takase, K., Chono, S., Ichion, E., Ogura, A., & Tanaka, K. (2017). Influence of topography and forest characteristics on snow distributions in a forested catchment. *Journal of Hydrology*, *546*, 289–298. https://doi.org/10.1016/j.jhydrol.2017.01.021

Gary, H. L. (1974). Snow accumulation and snowmelt as influenced by a small clearing in a lodgepole pine forest. *Water Resources Research*, *10*(2), 348–353. https://doi.org/10.1029/WR010i002p00348

Gauthier, S., Bernier, P., Kuuluvainen, T., Shvidenko, A. Z., & Schepaschenko, D. G. (2015). Boreal forest health and global change. *Science*, *349*(6250), 819–822. https://doi.org/10.1126/science.aaa9092

Gelfan, A. N., Pomeroy, J. W., & Kuchment, L. S. (2004). Modeling forest cover influences on snow accumulation, sublimation, and melt. *Journal of Hydrometeorology*, *5*(5), 785–803. https://doi.org/10.1175/1525-7541(2004)005<0785:MFCIOS>2.0.CO;2

Godsey, S. E., Kirchner, J. W., & Tague, C. L. (2014). Effects of changes in winter snowpacks on summer low flows: Case studies in the Sierra Nevada, California, USA. *Hydrological Processes*, *28*(19), 5048–5064. https://doi.org/10.1002/hyp.9943

Golding, D. L., & Swanson, R. H. (1978). Snow accumulation and melt in small forest openings in Alberta. *Canadian Journal of Forest Research*, *8*(4), 380–388. https://doi.org/10.1139/x78-057

Gray, Don M. (1978). Snow Accumulation and Distribution. In S. Colbeck (Ed.), *Proceedings of a meeting on Modelling Snow Cover Runoff* (pp. 359–368). U.S. Army Corps of Engineering. Cold Regions Research and Engineering Laboratory.

Gusmeroli, A., & Grosse, G. (2012). Ground penetrating radar detection of subsnow slush on ice-covered lakes in interior Alaska. *The Cryosphere*, *6*(6), 1435–1443. https://doi.org/10.5194/tc-6-1435-2012

Haberkorn, A. (Ed.). (2019). *European Snow Booklet*. https://doi.org/doi:10.16904/envidat.59

Harder, P., Pomeroy, J. W., & Helgason, W. D. (2020). Improving sub-canopy snow depth mapping with unmanned aerial vehicles: lidar versus structure-from-motion techniques. *The Cryosphere*, *14*(6), 1919–1935. https://doi.org/10.5194/tc-14-1919-2020

Hardy, J. P., Davis, R. E., Jordan, R., Li, X., Woodcock, C., Ni, W., & McKenzie, J. C. (1997). Snow ablation modeling at the stand scale in a boreal jack pine forest. *Journal of Geophysical Research: Atmospheres*, *102*(D24), 29397–29405. https://doi.org/10.1029/96JD03096

Hastie, T., Friedman, J., & Tibshirani, R. (2001). *The elements of statistical learning*. In Springer Series in Statistics. Springer New York. https://doi.org/10.1007/978-0-387-21606-5

Hastie, T., & Tibshirani, R. (1990). *Generalized Additive Models*. Monographs on Statistics and Applied Probability Series, 43. Chapman and Hall/CRC.

Hedstrom, N. R., & Pomeroy, J. W. (1998). Measurements and modelling of snow interception in the boreal forest. *Hydrological Processes*, *12*(10–11), 1611–1625. https://doi.org/10.1002/(SICI)1099-1085(199808/09)12:10/11<1611::AID-HYP684>3.0.CO;2-4

Hiemstra, C. A., Liston, G. E., & Reiners, W. A. (2002). Snow Redistribution by Wind and Interactions with Vegetation at Upper Treeline in the Medicine Bow Mountains, Wyoming, U.S.A. *Arctic, Antarctic, and Alpine Research*, *34*(3), 262–273. https://doi.org/10.1080/15230430.2002.12003493

Hock, R. (2003). Temperature index melt modelling in mountain areas. *Journal of Hydrology*, *282*(1–4), 104–115. https://doi.org/10.1016/S0022-1694(03)00257-9

Holden, J., Chapman, P. J., & Labadz, J. C. (2004). Artificial drainage of peatlands: hydrological and hydrochemical process and wetland restoration. *Progress in Physical Geography: Earth and Environment*, *28*(1), 95–123. https://doi.org/10.1191/0309133304pp403ra

Jenicek, M., Seibert, J., Zappa, M., Staudinger, M., & Jonas, T. (2016). Importance of maximum snow accumulation for summer low flows in humid catchments. *Hydrology and Earth System Sciences*, *20*(2), 859–874. https://doi.org/10.5194/hess-20-859-2016

Jost, G., Weiler, M., Gluns, D. R., & Alila, Y. (2007). The influence of forest and topography on snow accumulation and melt at the watershed-scale. *Journal of Hydrology*, *347*(1–2), 101–115. https://doi.org/10.1016/j.jhydrol.2007.09.006

Karlsen, R. H., Grabs, T., Bishop, K., Buffam, I., Laudon, H., & Seibert, J. (2016). Landscape controls on spatiotemporal discharge variability in a boreal catchment. *Water Resources Research*, *52*(8), 6541–6556. https://doi.org/10.1002/2016WR019186

Kelly, C. N., Mcguire, K. J., Miniat, C. F., & Vose, J. M. (2016). Extremes Altered By Forest Management. *Geophysical Research Letters*, *43*, 1–10. https://doi.org/10.1002/2016GL068058

Ketcheson, S. J., Whittington, P. N., & Price, J. S. (2012). The effect of peatland harvesting on snow accumulation, ablation and snow surface energy balance. *Hydrological Processes*, *26*(17), 2592–2600. https://doi.org/10.1002/hyp.9325

Kinar, N. J., & Pomeroy, J. W. (2015). Reviews of Geophysics Measurement of the physical properties of the snowpack. *Reviews of Geophysics*, *53*, 481–544. https://doi.org/10.1002/2015RG000481.Received

Kirchner, J. W. (2009). Catchments as simple dynamical systems: Catchment characterization, rainfall-runoff modeling, and doing hydrology backward. *Water Resources Research*, *45*(2), 1–34. https://doi.org/10.1029/2008WR006912

Konikow, L. F., & Kendy, E. (2005). Groundwater depletion: A global problem. *Hydrogeology Journal*, *13*(1), 317–320. https://doi.org/10.1007/s10040-004-0411-8

Koskinen, J. T., Pulliainen, J. T., & Hallikainen, M. T. (1997). The use of ers-1 sar data in snow melt monitoring. *IEEE Transactions on Geoscience and Remote Sensing*, *35*(3), 601–610. https://doi.org/10.1109/36.581975

Kozii, N., Laudon, H., Ottosson-Löfvenius, M., & Hasselquist, N. J. (2017). Increasing water losses from snow captured in the canopy of boreal forests: A case study using a 30 year data set. *Hydrological Processes*, *31*(20), 3558–3567. https://doi.org/10.1002/hyp.11277

Kumar, S., Zwiers, F., Dirmeyer, P. A., Lawrence, D. M., Shrestha, R., & Werner, A. T. (2016). Terrestrial contribution to the heterogeneity in hydrological changes under global warming. *Water Resources Research*, *52*(4), 3127–3142. https://doi.org/10.1002/2016WR018607

Kuusisto, E. (1984). Snow accumulation and snowmelt in Finland. In *Publications of the Water Research Institute* (Vol. 55). National Board of Waters. https://helda.helsinki.fi/handle/10138/31432

Lendzioch, T., Langhammer, J., & Jenicek, M. (2016). Tracking forest and open area effects on snow accumulation by unmanned aerial vehicle photogrammetry. *International Archives of the Photogrammetry, Remote Sensing and Spatial Information Sciences - ISPRS Archives*, *2016-Janua*(July), 917–923. https://doi.org/10.5194/isprsarchives-XLI-B1-917-2016

Li, Q., Wei, X., Yang, X., Giles-Hansen, K., Zhang, M., & Liu, W. (2018). Topography significantly influencing low flows in snow-dominated watersheds. *Hydrology and Earth System Sciences*, *22*(3), 1947–1956. https://doi.org/10.5194/hess-22-1947-2018

Lievens, H., Demuzere, M., Marshall, H. P., Reichle, R. H., Brucker, L., Brangers, I., de Rosnay, P., Dumont, M., Girotto, M., Immerzeel, W. W., Jonas, T., Kim, E. J., Koch, I., Marty, C., Saloranta, T., Schöber, J., & De Lannoy, G. J. M. (2019). Snow depth variability in the Northern Hemisphere mountains observed from space. *Nature Communications*, *10*(1), 1–12. https://doi.org/10.1038/s41467-019-12566-y

Link, T. E., & Marks, D. (1999). Point simulation of seasonal snow cover dynamics beneath boreal forest canopies. *Journal of Geophysical Research: Atmospheres*, *104*(D22), 27841–27857. https://doi.org/10.1029/1998JD200121

Liston, G. E. (1999). Interrelationships among snow distribution, snowmelt, and snow cover depletion: Implications for atmospheric, hydrologic, and ecologic modeling. *Journal of Applied Meteorology*, *38*(10), 1474–1487. https://doi.org/10.1175/1520-0450(1999)038<1474:IASDSA>2.0.CO;2

Liston, G. E. (2004). Representing subgrid snow cover heterogeneities in regional and global models. *Journal of Climate*, *17*(6), 1381–1397. https://doi.org/10.1175/1520-0442(2004)017<1381:RSSCHI>2.0.CO;2

Liston, G. E., & Sturm, M. (1998). A snow-transport model for complex terrain. *Journal of Glaciology*, *44*(148), 498–516. https://doi.org/10.3189/S0022143000002021

Liston, G. E., & Sturm, M. (2002). Winter precipitation patterns in arctic Alaska determined from a blowing-snow model and snow-depth observations. *Journal of Hydrometeorology*, *3*(6), 646–659. https://doi.org/10.1175/1525-7541(2002)003<0646:WPPIAA>2.0.CO;2

López-Moreno, J. I., Revuelto, J., Fassnacht, S. R., Azorín-Molina, C., Vicente-Serrano, S. M., Morán-Tejeda, E., & Sexstone, G. A. (2015). Snowpack variability across various spatio-temporal resolutions. *Hydrological Processes*, *29*(6), 1213–1224. https://doi.org/10.1002/hyp.10245

Lundberg, A., Granlund, N., & Gustafsson, D. (2010). Towards automated "ground truth" snow measurements-a review of operational and new measurement methods for Sweden, Norway, and Finland. *Hydrological Processes*, *24*(14), 1955–1970. https://doi.org/10.1002/hyp.7658

Lundquist, J. D., Dickerson-Lange, S. E., Lutz, J. A., & Cristea, N. C. (2013). Lower forest density enhances snow retention in regions with warmer winters: A global framework developed from plot-scale observations and modeling. *Water Resources Research*, *49*(10), 6356–6370. https://doi.org/10.1002/wrcr.20504

Lundquist, J. D., & Lott, F. (2008). Using inexpensive temperature sensors to monitor the duration and heterogeneity of snow-covered areas. *Water Resources Research*, *44*(4), 8–13. https://doi.org/10.1029/2008WR007035

Lundquist, J. D., & Lott, F. (2010). Using inexpensive temperature sensors to monitor the duration and heterogeneity of snow-covered areas. *Water Resources Research*, *46*(4), 8–13. https://doi.org/10.1029/2008WR007035

Luomaranta, A., Aalto, J., & Jylhä, K. (2019). Snow cover trends in Finland over 1961–2014 based on gridded snow depth observations. *International Journal of Climatology*, *39*(7), 3147–3159. https://doi.org/10.1002/joc.6007

Mankin, J. S., Viviroli, D., Singh, D., Hoekstra, A. Y., & Diffenbaugh, N. S. (2015). The potential for snow to supply human water demand in the present and future. *Environmental Research Letters*, *10*(11). https://doi.org/10.1088/1748-9326/10/11/114016

McKay, G. A., & Male, D. H. (1981). The distribution of snow cover. In D.M. Gray & D. H. Male (Eds.), *Handbook of Snow: Principles, Processes, Management, and Use* (pp. 153–190). Pergamon Press, Toronto, Canada.

Mudryk, L., Santolaria-Otín, M., Krinner, G., Ménégoz, M., Derksen, C., Brutel-Vuilmet, C., Brady, M., & Essery, R. (2020). Historical Northern Hemisphere snow cover trends and projected changes in the CMIP6 multi-model ensemble. *The Cryosphere*, *14*(7), 2495–2514. https://doi.org/10.5194/tc-14-2495-2020

Musselman, K. N., Clark, M. P., Liu, C., Ikeda, K., & Rasmussen, R. (2017). Slower snowmelt in a warmer world. *Nature Climate Change*, *7*(3), 214–219. https://doi.org/10.1038/nclimate3225

Musselman, K. N., Molotch, N. P., & Brooks, P. D. (2008). Effects of vegetation on snow accumulation and ablation in a mid-latitude sub-alpine forest. *Hydrological Processes*, *22*(15), 2767–2776. https://doi.org/10.1002/hyp.7050

Mustonen, K.-R., Mykrä, H., Marttila, H., Sarremejane, R., Veijalainen, N., Sippel, K., Muotka, T., & Hawkins, C. P. (2018). Thermal and hydrologic responses to climate change predict marked alterations in boreal stream invertebrate assemblages. *Global Change Biology*, *24*(6), 2434–2446. https://doi.org/10.1111/gcb.14053

National Land Survey of Finland. (2013). *Elevation model 10 m [Data file]*. https://tiedostopalvelu.maanmittauslaitos.fi/tp/kartta?lang=en

National Land Survey of Finland. (2020a). *Hillshade Shaded relief 8 m [Data file]*. https://tiedostopalvelu.maanmittauslaitos.fi/tp/kartta?lang=en

National Land Survey of Finland. (2020b). *Orthophoto [Data file]*. https://tiedostopalvelu.maanmittauslaitos.fi/tp/kartta?lang=en

Neumann, N. N., Derksen, C., Smith, C., & Goodison, B. (2006). Characterizing local scale snow cover using point measurements during the winter season. *Atmosphere - Ocean*, *44*(3), 257–269. https://doi.org/10.3137/ao.440304

Neuvonen, M., Sievänen, T., Fronzek, S., Lahtinen, I., Veijalainen, N., & Carter, T. R. (2015). Vulnerability of cross-country skiing to climate change in Finland – An interactive mapping tool. *Journal of Outdoor Recreation and Tourism*, *11*, 64–79. https://doi.org/10.1016/j.jort.2015.06.010

Niedzielski, T., Szymanowski, M., Miziński, B., Spallek, W., Witek-Kasprzak, M., Ślopek, J., Kasprzak, M., Błaś, M., Sobik, M., Jancewicz, K., Borowicz, D., Remisz, J., Modzel, P., Męcina, K., & Leszczyński, L. (2019). Estimating snow water equivalent using unmanned aerial vehicles for determining snow-melt runoff. *Journal of Hydrology*, *578*(July), 124046. https://doi.org/10.1016/j.jhydrol.2019.124046

Nolin, A. W. (2011). Recent advances in remote sensing of seasonal snow. *Journal of Glaciology*, *56*(200), 1141–1150. https://doi.org/10.3189/002214311796406077

Okkonen, J., & Kløve, B. (2010). A conceptual and statistical approach for the analysis of climate impact on ground water table fluctuation patterns in cold conditions. *Journal of Hydrology*, *388*(1–2), 1–12. https://doi.org/10.1016/j.jhydrol.2010.02.015

Okkonen, J., & Kløve, B. (2011). A sequential modelling approach to assess groundwater–surface water resources in a snow dominated region of Finland. *Journal of Hydrology*, *411*(1–2), 91–107. https://doi.org/10.1016/j.jhydrol.2011.09.038

Payn, R. A., Gooseff, M. N., McGlynn, B. L., Bencala, K. E., & Wondzell, S. M. (2012). Exploring changes in the spatial distribution of stream baseflow generation during a seasonal recession. *Water Resources Research*, *48*(4), 1–15. https://doi.org/10.1029/2011WR011552

Peel, M. C., Finlayson, B. L., & McMahon, T. A. (2007). Updated world map of the Köppen-Geiger climate classification. *Hydrology and Earth System Sciences*, *11*(5), 1633–1644. https://doi.org/10.5194/hess-11-1633-2007

Pirazzini, R., Leppänen, L., Picard, G., Lopez-Moreno, J. I., Marty, C., Macelloni, G., Kontu, A., von Lerber, A., Tanis, C. M., Schneebeli, M., de Rosnay, P., & Arslan, A. N. (2018). European In-Situ Snow Measurements: Practices and Purposes. *Sensors*, *18*(7), 2016. https://doi.org/10.3390/s18072016

Pirinen, P., Simola, H., Aalto, J., Kaukoranta, J.-P., Karlsson, P., & Reija, R. (2012). Climatological statistics of Finland 1981–2010. In *Finnish Meteorological Reports* (Vol. 1). Finnish Meteorological Institute. https://helda.helsinki.fi/handle/10138/35880

Poff, N. L., Allan, J. D., Bain, M. B., Karr, J. R., Prestegaard, K. L., Richter, B. D., Sparks, R. E., & Stromberg, J. C. (1997). The Natural Flow Regime. *BioScience*, *47*(11), 769–784. https://doi.org/10.2307/1313099

Pomeroy, J. W., & Dion, K. (1996). Winter radiation extinction and reflectioin in a boreal pine canopy: Measurements and modelling. *Hydrological Processes*, *10*(12), 1591–1608. https://doi.org/10.1002/(SICI)1099-1085(199612)10:12<1591::AID-HYP503>3.0.CO;2-8

Pomeroy, J. W., & Goodison, B. E. (1997). Winter and snow. In W. G. Bailey, R. O. Timothy, & W. R. Rouse (Eds.), *The Surface Climates of Canada* (pp. 68–100). McGill/Queen's University Press.

Pomeroy, J. W., & Gray, D. M. (1995). Snowcover-accumulation, relocation and management. In *National Hydrology Research Institute science report* (Issue 7). National Hydrology Research Institute.

Pomeroy, J. W., Gray, D. M., Hedstrom, N. R., & Janowicz, J. R. (2002). Prediction of seasonal snow accumulation in cold climate forests. *Hydrological Processes*, *16*(18), 3543–3558. https://doi.org/10.1002/hyp.1228

Prévost, M., Plamondon, A. P., & Belleau, P. (1999). Effects of drainage of a forested peatland on water quality and quantity. *Journal of Hydrology*, *214*(1–4), 130–143. https://doi.org/10.1016/S0022-1694(98)00281-9

Price, K. (2011). Effects of watershed topography, soils, land use, and climate on baseflow hydrology in humid regions: A review. *Progress in Physical Geography*, *35*(4), 465–492. https://doi.org/10.1177/0309133311402714

Prowse, T., Bring, A., Mård, J., Carmack, E., Holland, M., Instanes, A., Vihma, T., & Wrona, F. J. (2015). Arctic Freshwater Synthesis: Summary of key emerging issues. *Journal of Geophysical Research: Biogeosciences*, *120*(10), 1887–1893. https://doi.org/10.1002/2015JG003128

Pulliainen, J., Luojus, K., Derksen, C., Mudryk, L., Lemmetyinen, J., Salminen, M., Ikonen, J., Takala, M., Cohen, J., Smolander, T., & Norberg, J. (2020). Patterns and trends of Northern Hemisphere snow mass from 1980 to 2018. *Nature*, *581*(7808), 294–298. https://doi.org/10.1038/s41586-020-2258-0

Räisänen, J. (2016). Twenty-first century changes in snowfall climate in Northern Europe in ENSEMBLES regional climate models. *Climate Dynamics*, *46*(1–2), 339–353. https://doi.org/10.1007/s00382-015-2587-0

Räisänen, J., & Eklund, J. (2012). 21st Century changes in snow climate in Northern Europe: a high-resolution view from ENSEMBLES regional climate models. *Climate Dynamics*, *38*(11–12), 2575–2591. https://doi.org/10.1007/s00382-011-1076-3

Rasmus, S. (2005). Snow pack structure characteristics in Finland - measurements and modelling. In *Report series in Geophysics* (Issue 48). University of Helsinki. https://helda.helsinki.fi/handle/10138/23226

Rauhala, A., Meriö, L.-J., Ala-aho, P., Korpelainen, P., Kuzmin, A., Kumpula, T., Heikkilä, R., Klöve, B., & Marttila, H. (2021). *Spatiotemporal Variability of Snow Depth in Subarctic Environment Using Unmanned Aircraft Systems, Part 1: Measurements, Processing, and Accuracy Assessment. Unpublished manuscript.*

Redpath, T. A. N., Sirguey, P., & Cullen, N. J. (2018). Repeat mapping of snow depth across an alpine catchment with RPAS photogrammetry. *Cryosphere*, *12*(11), 3477–3497. https://doi.org/10.5194/tc-12-3477-2018

Reusser, D. E., & Zehe, E. (2011). Low-cost monitoring of snow height and thermal properties with inexpensive temperature sensors. *Hydrological Processes*, *25*(12), 1841–1852. https://doi.org/10.1002/hyp.7937

Rice, R., & Bales, R. C. (2010). Embedded-sensor network design for snow cover measurements around snow pillow and snow course sites in the Sierra Nevada of California. *Water Resources Research*, *46*(3), 1–13. https://doi.org/10.1029/2008WR007318

Sandvik, B. (2009). *World Borders Dataset [Data file]*. http://thematicmapping.org/downloads/world_borders.php

Scott, D., Dawson, J., & Jones, B. (2008). Climate change vulnerability of the US Northeast winter recreation– tourism sector. *Mitigation and Adaptation Strategies for Global Change*, *13*(5–6), 577–596. https://doi.org/10.1007/s11027-007-9136-z

Seuna, P. (1983). Small basins - A tool in scientific and operational hydrology. In *Publications of the Water Research Institute*. National Board of Waters, Finland. https://helda.helsinki.fi/handle/10138/31417

Shook, K., & Gray, D. M. (1996). Small-scale spatial structure of shallow snowcovers. *Hydrological Processes*, *10*(10), 1283–1292. https://doi.org/10.1002/(SICI)1099-1085(199610)10:10<1283::AID-HYP460>3.0.CO;2-M

Sørensen, R., Ring, E., Meili, M., Högbom, L., Seibert, J., Grabs, T., Laudon, H., & Bishop, K. (2009). Forest Harvest Increases Runoff Most during Low Flows in Two Boreal Streams. *AMBIO: A Journal of the Human Environment*, *38*(7), 357–363. https://doi.org/10.1579/0044-7447-38.7.357

Staudinger, M., Stoelzle, M., Seeger, S., Seibert, J., Weiler, M., & Stahl, K. (2017). Catchment water storage variation with elevation. *Hydrological Processes*, *31*(11), 2000–2015. https://doi.org/10.1002/hyp.11158

Stocker, T. F., Qin, D., Plattner, G.-K., Tignor, M., Allen, S. K., Boschung, J., Nauels, A., Xia, Y., Bex, V., & Midgley, P. M. (Eds.). (2014). Summary for Policymakers. In *Climate Change 2013: The Physical Science Basis. Contribution of Working Group I to the Fifth Assessment Report of the Intergovernmental Panel on Climate Change* (pp. 1–30). Cambridge University Press.

Sturm, M. (2015). White water: Fifty years of snow research in WRR and the outlook for the future. *Water Resources Research*, *51*(7), 4948–4965. https://doi.org/10.1002/2015WR017242

Sturm, M., Goldstein, M. A., & Parr, C. (2017). Water and life from snow: A trillion dollar science question. *Water Resources Research*, *53*(5), 3534–3544. https://doi.org/10.1002/2017WR020840

Sturm, M., & Holmgren, J. (2018). An Automatic Snow Depth Probe for Field Validation Campaigns. *Water Resources Research*, *54*(11), 9695–9701. https://doi.org/10.1029/2018WR023559

Sun, S., Chen, H., Ju, W., Song, J., Zhang, H., Sun, J., & Fang, Y. (2013). Effects of climate change on annual streamflow using climate elasticity in Poyang Lake Basin, China. *Theoretical and Applied Climatology*, *112*(1–2), 169–183. https://doi.org/10.1007/s00704-012-0714-y

Sutinen, R., Äikää, O., Piekkari, M., & Hänninen, P. (2009). Snowmelt infiltration through partially frozen soil in Finnish Lapland. *Geophysica*, *45*(1–2), 27–39.

Sutinen, R., Hänninen, P., & Venäläinen, A. (2008). Effect of mild winter events on soil water content beneath snowpack. *Cold Regions Science and Technology*, *51*(1), 56–67. https://doi.org/10.1016/j.coldregions.2007.05.014

Sutinen, R., Närhi, P., Middleton, M., Hänninen, P., Timonen, M., & Sutinen, M.-L. (2012). Advance of Norway spruce (Picea abies) onto mafic Lommoltunturi fell in Finnish Lapland during the last 200 years. *Boreas*, *41*(3), 367–378. https://doi.org/10.1111/j.1502-3885.2011.00238.x

Talbot, J., Plamondon, A. P., Lévesque, D., Aubé, D., Prévos, M., Chazalmartin, F., & Gnocchini, M. (2006). Relating snow dynamics and balsam fir stand characteristics, Montmorency Forest, Quebec. *Hydrological Processes*, *20*(5), 1187–1199. https://doi.org/10.1002/hyp.5938

Vajda, A., Venäläinen, A., Hänninen, P., & Sutinen, R. (2006). Effect of vegetation on snow cover at the northern timberline: A case study in Finnish Lapland. *Silva Fennica*, *40*(2), 195–207.

Vander Jagt, B., Lucieer, A., Wallace, L., Turner, D., & Durand, M. (2015). Snow depth retrieval with UAS using photogrammetric techniques. *Geosciences (Switzerland)*, *5*(3), 264–285. https://doi.org/10.3390/geosciences5030264

Varhola, A., Coops, N. C., Weiler, M., & Moore, R. D. (2010). Forest canopy effects on snow accumulation and ablation: An integrative review of empirical results. *Journal of Hydrology*, *392*(3–4), 219–233. https://doi.org/10.1016/j.jhydrol.2010.08.009

Vörösmarty, C. J., McIntyre, P. B., Gessner, M. O., Dudgeon, D., Prusevich, A., Green, P., Glidden, S., Bunn, S. E., Sullivan, C. A., Liermann, C. R., & Davies, P. M. (2010). Global threats to human water security and river biodiversity. *Nature*, *467*(7315), 555–561. https://doi.org/10.1038/nature09440

Wada, Y., van Beek, L. P. H., van Kempen, C. M., Reckman, J. W. T. M., Vasak, S., & Bierkens, M. F. P. (2010). Global depletion of groundwater resources. *Geophysical Research Letters*, *37*(20). https://doi.org/10.1029/2010GL044571

Waddington, J. M., Morris, P. J., Kettridge, N., Granath, G., Thompson, D. K., & Moore, P. A. (2015). Hydrological feedbacks in northern peatlands. *Ecohydrology*, *8*(1), 113–127. https://doi.org/10.1002/eco.1493

Walker, B., Wilcox, E. J., & Marsh, P. (2020). Accuracy assessment of late winter snow depth mapping for tundra environments using Structure-from-Motion photogrammetry. *Arctic Science*, AS-2020-0006. https://doi.org/10.1139/AS-2020-0006

Webb, R. W. (2017). Using ground penetrating radar to assess the variability of snow water equivalent and melt in a mixed canopy forest, Northern Colorado. *Frontiers of Earth Science*, *11*(3), 482–495. https://doi.org/10.1007/s11707-017-0645-0

Westoby, M. J., Brasington, J., Glasser, N. F., Hambrey, M. J., & Reynolds, J. M. (2012). 'Structure-from-Motion' photogrammetry: A low-cost, effective tool for geoscience applications. *Geomorphology*, *179*, 300–314. https://doi.org/10.1016/j.geomorph.2012.08.021

Whitehead, P. G., Wilby, R. L., Battarbee, R. W., Kernan, M., & Wade, A. J. (2009). A review of the potential impacts of climate change on surface water quality. *Hydrological Sciences Journal*, *54*(1), 101–123. https://doi.org/10.1623/hysj.54.1.101

Winstral, A., & Marks, D. (2014). Long-term snow distribution observations in a mountain catchment: Assessing variability, time stability, and the representativeness of an index site. *Water Resources Research*, *50*(1), 293–305. https://doi.org/10.1002/2012WR013038

Winter, T. C., & Woo, M.-K. (1990). Hydrology of lakes and wetlands. In *Surface Water Hydrology*. Geological Society of America. https://doi.org/10.1130/DNAG-GNA-O1.159

Woo, M. K., Thorne, R., Szeto, K., & Yang, D. (2008). Streamflow hydrology in the boreal region under the influences of climate and human interference. *Philosophical Transactions of the Royal Society B: Biological Sciences*, *363*(1501), 2251–2260. https://doi.org/10.1098/rstb.2007.2197

Woods, R. (2005). Hydrologic Concepts of Variability and Scale. In *Encyclopedia of Hydrological Sciences*. John Wiley & Sons, Ltd. https://doi.org/10.1002/0470848944.hsa002

# Original publications

I Meriö, L.-J., Marttila, H., Ala-aho, P., Hänninen, P., Okkonen, J., Sutinen, R., & Kløve, B. (2018). Snow profile temperature measurements in spatiotemporal analysis of snowmelt in a subarctic forest-mire hillslope. *Cold Regions Science and Technology, 151,* 119–132. https://doi.org/10.1016/j.coldregions.2018.03.013

II Meriö, L.-J., Rauhala, A., Ala-aho, P., Kuzmin, A., Korpelainen, P.,Kumpula, T., Kløve, B., & Marttila, H. (2021). Spatiotemporal variability of snow depth in subarctic environment using unmanned aircraft systems, Part 2: Snow processes and snow-canopy interactions. Manuscript.

III Meriö, L.-J., Ala-aho, P., Linjama, J., Hjort, J., Kløve, B., & Marttila, H. (2019). Snow to precipitation ratio controls catchment storage and summer flows in boreal headwater catchments. *Water Resources Research, 55*(5), 4096–4109. https://doi.org/10.1029/2018wr023031



Original publications are not included in the electronic version of the dissertation.

788. Tavakolian, Mohammad (2021) Efficient spatiotemporal representation learning for pain intensity estimation from facial expressions

789. Longi, Henna (2021) Regional innovation systems and company engagement in the Arctic context

790. Moltafet, Mohammad (2021) Information freshness in wireless networks

791. Nevanperä, Tuomas (2021) Catalytic oxidation of harmful chlorine- and sulphur-containing VOC emissions : a study of supported Au, Pt and Cu catalysts

792. Baharmast, Aram (2021) Wide dynamic range CMOS receiver techniques for a pulsed Time-of-Flight laser rangefinder

793. Haiko, Oskari (2021) Effect of microstructural characteristics and mechanical properties on the impact-abrasive and abrasive wear resistance of ultra-high strength steels

794. Oppenlaender, Jonas (2021) Crowdsourcing creative work

795. Kimbi Yaah, Velma Beri (2021) Development of novel biomass-based materials for the treatment of emerging contaminants in water

796. Liu, Chen-Feng (2021) Resource allocation for ultra-reliable and low-latency 5G communication

797. Kilpijärvi, Joni (2021) RF-microwave sensor development for cell and human in vitro and ex vivo monitoring

798. Huikari, Jaakko (2021) 2D CMOS SPAD array techniques in 1D pulsed TOF distance measurement applications

799. Peyvasteh, Motahareh (2021) Polarimetric and spectral imaging approaches for quantitative characterization of inhomogeneous scattering media including biotissues

800. Shehab, Mohammad (2021) Energy efficient QoS provisioning and resource allocation for machine type communication

801. Jounila, Henri (2021) Integroidulla HSEQ-johtamisella kokonaisvaltaista yritysvastuullisuutta : tapaustutkimuksia yritysten työturvallisuuden ja HSEQ:n kehittämisestä

802. Nellattukuzhi Sreenivasan, Harisankar (2021) Synthesis and alkali activation of Magnesium-rich aluminosilicates

803. Kallio, Johanna (2021) Unobtrusive stress assessment in knowledge work using real-life environmental sensor data

Book orders:
Virtual book store
http://verkkokauppa.juvenesprint.fi

UNIVERSITY OF OULU P.O. Box 8000 FI-90014 UNIVERSITY OF OULU FINLAND

# ACTA UNIVERSITATIS OULUENSIS



ISBN 978-952-62-3064-1 (Paperback)
ISBN 978-952-62-3065-8 (PDF)
ISSN 0355-3213 (Print)
ISSN 1796-2226 (Online)

UNIVERSITY OF OULU